EXPLORATION OF LABORATORY TECHNIQUES RELATING TO *CRYPTOSPORIDIUM*

PARVUM PROPAGATION, LIFE CYCLE OBSERVATION, AND HOST IMMUNE

RESPONSES TO INFECTION

A Thesis
Submitted to the Graduate Faculty
of the
North Dakota State University
of Agriculture and Applied Science

By

Cheryl Marie Brown

In Partial Fulfillment
for the Degree of
MASTER OF SCIENCE

Major Department:
Veterinary and Microbiological Sciences

February 2014

Fargo, North Dakota

North Dakota State University
Graduate School

Title

EXPLORATION OF LABORATORY TECHNIQUES RELATING TO
CRYPTOSPORIDIUM PARVUM PROPAGATION, LIFE CYCLE
OBSERVATION, AND HOST IMMUNE RESPONSES TO
INFECTION

By

Cheryl Marie Brown

The Supervisory Committee certifies that this ***disquisition*** complies
with North Dakota State University's regulations and meets the accepted
standards for the degree of

MASTER OF SCIENCE

SUPERVISORY COMMITTEE:

 Dr. Jane Schuh
Chair

Dr. John McEvoy

Dr. Carrie Hammer

Approved:

4-8-14	Dr. Charlene Wolf-Hall
Date	Department Chair

ii

ABSTRACT

Cryptosporidium causes cryptosporidiosis, a self-limiting diarrheal disease in healthy people, but causes serious health issues for immunocompromised individuals. Cryptosporidiosis has been observed in humans since the early 1970s and continues to cause public health concerns. *Cryptosporidium* has a complicated life cycle making laboratory study challenging. This project explores several ways of studying *Cryptosporidium parvum,* with a goal of applying existing techniques to further understand this life cycle. Utilization of a neonatal mouse model demonstrated laser microdissection as a tool for studying host immune response to infeciton. A cell culture technique developed on FrameSlides™ enables laser microdissection of individual infected cells for further analysis. Finally, the hypothesis that the availability of cells to infect drives the switch from asexual to sexual parasite reproduction was tested by time-series infection. The results suggest this isn't accurate. These experiments open the door to several avenues of *Cryptosporidium* study and the host response to cryptosporidiosis.

ACKNOWLEDGMENTS

DEDICATION

I would have loved to have had one more chance to thank Dr. David Berryhill face-to-face for his ongoing support and encouragement and pep talks when things got stinky. Doc, you may be gone, but you are not forgotten! I still half expect to bump into you on one of your wanders when I come around corners in Van Es!

This thesis is dedicated to my loving family and to my darling Monkeys.

It is finished.

We will never speak of this again.

TABLE OF CONTENTS

LIST OF TABLES

LIST OF FIGURES

LITERATURE REVIEW

Thesis outline

When starting to work on *Cryptosporidium*, two things were evident. First, cryptosporidiosis is a disease of increasing importance. In immunocompetent individuals, it is normally a self-limiting disease, but can be one of life-threatening impact as more and more individuals live longer with compromised immunity. Next, there is a great deal left to be discovered about *Cryptosporidium sp.* due to a complex life cycle that hampers many of the fundamental characterizations that are available for most pathogens.

This thesis is structured in two parts. It will thoroughly review the available *Cryptosporidium* literature, describing the taxonomy and biology of the parasite itself, as well as the disease that it causes and treatment options. A description of past and future research will be presented, highlighting the challenges faced by researchers investigating this unique organism. While many of the experiments that are illustrated in this manuscript will need further modification, they represent my contribution to providing research tools to further this field of research.

Introduction

Discovered in 1907 in the gastric glands and ilea of mice (Tyzzer, 1907, 1910), *Cryptosporidium* was not recognized as a human pathogen until 1973, when an immunocompetent child presented with gastroenteritis and *Cryptosporidium* oocysts in his stools (Nime, 1976). Cryptosporidiosis is a disease caused by the *Cryptosporidium* parasite and is marked by severe, watery diarrhea that, in otherwise healthy humans or other animals, can last up to two weeks (O'Donoghue, 1995). Infected individuals may also have severe cramping, nausea, vomiting, dehydration, and fever (Thompson et al., 2005). Cryptosporidiosis can be life threatening in immunocompromised patients, and it has

become a major public health concern particularly in HIV-infected individuals living with compromised immune systems (Casemore, 1985, Guerrant, 1997). Two species of *Cryptosporidium* are known to cause the majority of cases of human cryptosporidiosis; *Cryptosporidium hominis*, which primarily infects only humans, and *Cryptosporidium parvum*, which can infect humans as well as several domestic animal species, including cattle (Ernest, et al., 1986., Zu, et al., 1992).

Nitazoxanide is currently used to treat cryptosporidiosis in immunocompetent patients, ameliorating symptoms and decreasing parasite-clearance time, but chemotherapeutic options for treating chronic cryptosporidiosis are limited in patients with poor immune systems (Blagburn, Soave 1997, Rossignol, 2010). For example, nitazoxanide has proved to be ineffective in AIDS patients with very low T cell counts. To improve efficacy, HIV-positive patients must first undergo highly active anti-retrovirus (HAART) treatment to restore immune function (Amadi, B., et al., 2002, Gomez-Morales, 2004). Current research exploring new chemical derivatives of Nitazoxanide shows increased anti-cryptosporidial action, even in immunocompromised hosts (Gargala, et al., 2010, Gargala, 2008, Ballard, et al., 2010).

Basic research and potential treatment advances are hindered by the complex life cycle of the parasite, which limits *in vivo* modeling, and the lack of an effective method for its propagation *in vitro*. *In vivo* models are limited to larger young animals, such as a calf, which can provide a sustained *C. parvum* infection and a short-term mouse model, which can be used for limited propagation. Unfortunately, each has major drawbacks. Calves are large and expensive research animals, which are not easily housed in laboratory environments. *C. hominis* infects only humans, which is one reason that *C.* parvum is used frequently in lab study. Neonatal and genetically immunocompromised mice that can be infected with *Cryptosporidium* sp. provide only a short temporal reflection of the parasite's interaction with the host. This model cannot replicate the disease process in the

context of a host response since the model necessitates the absence of a competent host response. The lack of an effective lab model is one of the largest challenges currently facing *Cryptosporidium* researchers.

Cryptosporidium classification and taxonomy

When E. E. Tyzzer first observed *Cryptosporidium* in the intestines and gastric ducts of mice, he classified it as a Coccidiomorpha in the phylum Sporozoa due to similarities in the life cycle of coccidian parasites. He named it *Cryptosporidium* due to the appearance of 'hidden' sporozoites in the infectious oocyst (Tyzzer, 1910). Tyzzer discussed the similarity of the newly identified organism's life cycle to gregarines in that the majority of these organisms' life cycles were spent either attached to the epithelial surface or free within the gastric glands and intestines. Although he did not think that the parasite penetrated the host cell, he classified it with the coccidians (Tyzzer, 1910). In addition, *Cryptosporidium* parasites possess a unique feeder organelle (Figure 1) that distinguishes it from other coccidians (Hampton and Rosario, 1966). It was not until 1996 that *Cryptosporidium* species were noted to be intracellular, but extracytoplasmic, parasites (Goodgame, 1996). Based on electron microscopic observations, the phylum has been changed to Apicomplexa (Levine, 1988). *Cryptosporidium* species are classified as follows in Table 1 (Fayer, 2008).

Table 1. Classification of *Cryptosporidium*

Kingdom	Eukaryota
Phylum	Protozoa
Subphylum	Apicomplexa
Class	Coccidia
Order	Eucoccidiorida
Family	Cryptosporidiidae
Genus	*Cryptosporidium*
Type Species	*C. parvum*

Figure 1. The unique feeder organelle of *Cryptosporidium sp.* The feeder organelle (arrow) is made up of lamella which becomes folded at the attachment site. The feeder organelle may function to provide sustenance for the developing stages of the parasite and to communicate between host and parasite. (Pohlenz, *et al.*, 1978).

Apicomplexans are characterized by the apical congregation of organelles that function in parasite motility and invasion of host cells during infection. *Cryptosporidium* sporozoites and merozoites, the cell-invading stages, possess an apical secretory complex that is typical of the phylum. In *Cryptosporidium*, this complex is made up of a single rhoptry and multiple micronemes. In collaboration with receptors on the host's cells (Langer and Riggs, 1999), proteins extruded from the apical secretory complex assist in attachment (Chen, et al., 2004) and help to remodel the host cell membrane into an intracellular, but extracytoplasmic, parasitophorous vacuole in which the parasite matures (O'Hara, et al., 2005).

Host-pathogen specificity was thought to be absolute, and as new strains were discovered, they were named based on their host and oocyst morphology. The need for more accurate species identification was obvious when it was recognized that a single *Cryptosporidium* species could infect multiple host species (Levine, 1988). Genetic analysis first utilized restriction fragment length polymorphism, identifying isolates based on variability in fragment lengths after cleavage with restriction enzymes, which allowed differentiation between species that had similar oocyst morphology and host affinity

(McLauchlin, et al., 2000; Xiao, et al., 2001). Several polymorphic loci have been identified by genome sequencing, making subgenotyping possible (Spano, et al., 1997; Xiao, et al., 1999). Polymorphic genes used to identify *Cryptosporidium* species include those for *Cryptosporidium* oocyst wall proteins (*COWP1* - 9), the*18S* small subunit (SSU) rRNA, thrombospondin-related adhesive protein (*TRAP*), and heat shock protein-70 (*HSP70*). These have been recognized as having distinct, species-specific differences (Templeton and Kaslow, 1997; Robson et al., 1998; Spano, et al., 1997). As genetic analysis has enabled more accurate classification of species, occasionally separately identified species have been consolidated to one species with a more diverse host range than originally reported (McLauchlin, et al., 2000; Kiao, et al., 2001). In contrast, some genotypes or subspecies have been reclassified as separate species when genetic analysis revealed that they were less closely related than assumed (Fayer, et al., 2008) or combined species or genotypes when differences between the organisms have not been great enough to maintain their status as discrete species.

The application of sequence analysis causes the number of recognized species and genotypes to adjust almost continually. In 2000, Fayer and colleagues (2000) published a report recognizing 10 species (Fayer, 2000). In 2004, Fayer recognized 15 species with multiple sub-types and sub-species (Fayer, 2004). The most recent classification of *Cryptosporidium* taxonomy lists 25 species and 40 genotypes (Fayer, 2010). The Fayer paper sets forth guidelines in classification and naming of new species of *Cryptosporidium*. Table 2 lists the currently recognized species, arranged by host type (Fayer, 2010).

The *Cryptosporidium* life cycle

Cryptosporidium has a complex life cycle, which includes an exogenous, infectious cycle and an endogenous, intracellular parasitic cycle. It undergoes both asexual and

sexual reproduction within its host. There is also research indicating that there may be extracellular life stages (Carreno, et al., 1999; Hijjawi, et al., 2002; Rosales, et al., 2005). Hijjawi has successfully cultured *Cryptosporidium* in host cell-free cultures, although this has proven difficult to replicate by other researchers (Hijjawi, et al., 2002; Girouard, 2006; Zhang, et al., 2009).

Cryptosporidium* is a monoxenous parasite, undergoing all life stages, including sexual and asexual reproduction, within a single host (O'Donoghue, 1995). The infectious, environmental oocyst stage is ingested by the host and contains four sporozoites (Ostrovska K. & Paperna I. 1990; Itakura, C., 1985). Asexual reproduction produces Type I meronts and allows the parasite to rapidly proliferate, and Type II meronts, which are believed to give rise to microgametes and macrogametes, which signal the start of sexual reproduction. When a microgamete fertilizes a macrogamete, a zygote is formed, which matures into an oocyst containing four sporozoites. There are two distinct types of oocysts: thin-walled oocysts that promote an autoinfection cycle and thick-walled, environmentally robust oocysts that are shed in the feces and that may infect new hosts (Current, 1985; Current & Reese, 1986). There are variations between species as to the site of infection within the host (Thompson, 2003; Xiao, 2004). *Cryptosporidium*'s life cycle is illustrated in Figure 2, and Table 3 lists species by their site of infection.

Ingestion, excystation, and attachment

Upon ingestion, the *Cryptosporidium* oocyst is able to resist the low pH of stomach acids and the chemical environment of digestive bile in its travel to the small intestine, where it excysts. Research suggests that the reducing conditions in the stomach and small intestine affect the oocyst wall, thinning it in preparation for excystation (Chen et al., 2004). In the intestine, terminal sialic acid residues on the epithelial cells of the small intestine react with receptors on the oocyst, triggering excystation (Choudhry, 2008). The layers of the oocyst peel back from the suture line and create an opening (Valigurová, A., et

6

al., 2008). Sporozoites escape through this opening and infect nearby epithelial cells(Reduker, et al., 1985; Fayer, et al., 1997; Smith, et al., 2005). An image of sporozoites escaping an oocyst is shown in Figure 3.

Table 2. *Cryptosporidium* species by host type

Cryptosporidium species reported from fish		
Species Name	Host (species)	Reference
C. molnari	*Sparus aurata* (Gilthead Seabream)	Alvarez-Pellitero and Sitja-Bobadilla (2002)
C. scophthalmi	Scophthalmi maximus (turbot)	Alvarez-Pellitero et al., (2004)
Cryptosporidium species reported from amphibian and reptiles		
Species Name	Host (species)	Reference
C. serpentis	Corn Snake (Elaphe guttata)	Levine (1980)
C. varanii	Emerald Monitor (Varanus prasinus)	Pavlásek et al. (1995)
C. fragile	Black-spined toad (Duttaphrynus melanostictus)	Jirku et al. (2008)
Cryptosporidium species reported from birds		
Species Name	Host (species)	Reference
C. meleagridis	Turkey (Meleagris gallopavo)	Slavin (1955)
C. baileyi	Chicken (Gallus gallus)	Current et al. (1986)
C. galli	Chicken (Gallus gallus)	Pavlásek (1999)
Cryptosporidium species reported from mammals		
Species Name	Host (species)	Reference
C. muris	Mouse (Mus musculus)	Tyzzer (1907)
C. parvum	Mouse (Mus musculus)	Tyzzer (1912)
C. wrairi	Guinea pig (Cavia porcellus)	Vetterling et al. (1971)
C. felis	Cat (Felis catis)	Iseki (1979)
C. andersoni	Cattle (Bos taurus)	Lindsay et al. (2000)
C. canis	Dog (Canis familiaris)	Fayer et al. (2001)
C. hominis	Human (Homo sapiens)	Morgan-Ryan et al. (2002)
C. suis	Pig (Sus scrofa)	Ryan et al. (2004a)
C. bovis	Cattle (Bos taurus)	Fayer et al. (2005)
C. fayeri	Kangaroo (Macropus rufus)	Ryan et al. (2008)
C. ryanae	Cattle (Bos taurus)	Fayer et al. (2008)
C. macropodum	Kangaroo (Macropus iganteus)	Power and Ryan (2008)

Figure 2. Schematic representation of *Cryptosporidium* life cycle. Both exogenous and endogenous, as well as sexual and asexual, stages are shown. Infectious oocysts are ingested and excyst within the small intestine. Sporozoites attach to host cells, becoming enveloped by host cell membrane. Trophozoites undergo merogony, developing into Type I or Type II meronts. Type I meronts produce 6-8 merozoites that go on to infect more cells, continuing the asexual reproductive stages. Type II meronts product 4 merozoites that infect more cells and differentiate into microgamonts and macrogamonts that carry out the sexual reproductive stage. Microgamonts product 16 microgametes, while macrogamonts develop into single-nucleated macrogametes. Microgametes attach and enter cells containing macrogametes and fertilization produces zygotes. The zygotes develop into oocysts containing 4 sporozoites. Thick-walled oocysts are shed in the feces. Thin-walled oocysts excyst within the host, and autoinfection continues the life cycle. (Adapted from Centers for Disease Control and Prevention, Current and Garcia 1991).

The gliding motility of sporozoites and merozoites is not fully understood. It is known that during the stages, when sporozoites or merozoites are employing gliding motility, the organelles in the apical complex extrude proteins that play a role in gliding motility. Actin polymerization and a myosin motor within the sporozoite function to move the sporozoite along the surface of the host cell. Receptors on the parasite attach to ligands on the host cell and are translocated by an actin/myosin complex to move it along (Sibley, 2004, Choudhry, 2008). The sporozoites orient themselves with their apical end towards the surface of the epithelial cells during invasion (Tzipori, 1998).

Table 3. List of *Cryptosporidium* species and site of infection

Species	Site of infection	Reference
C. andersoni	Stomach	[Lindsay, D.S., et al., 2000]
*C. baileyi**	Trachea, bursa of Fabricius, cloacae	[Current, W.L. et al.,1986]
C. bovis	Unknown	[Fayer, R. et al., 2005]
*C. canis**	Small intestine	[Fayer, R. et al.,2001]
C. fayeri	Unknown	[Ryan, et al., 2008]
*C. felis**	Small intestine	[Iseki, M.,1979]
C. fragile	Gastric	[Jirku, et al., 2008]
C. galli	Proventriculus	[Ryan, U.M. et al.,2003]
*C. hominis**	Small intestine	[Morgan-Ryan, U.M. et al.,2002]
C. macropodum	Unknown	[Power and Ryan, 2008]
*C. meleagridis**	Intestine	[Slavin, D.,1955]
C. molnari	Stomach	[Alvarez-Pellitero, P. and Sitja-Bobadilla, A.,2002]
*C. muris**	Stomach	[Tyzzer, E.E.,1907]
C. parvum	Small intestine	[Tyzzer, E.E.,1912]
C. ryanae	Unknown	[Fayer, R., et al., 2008]
C. saurophilum	Intestinal and cloacal mucosa	[Koudela, B. and Modry, D.,1998]
C. serpentis	Stomach	[Levine, N.D.,1980]
C. suis	Small intestine	[Ryan, U.M. et al.,2004]
C. varanii	Gastric	[Pavlásek, et al., 1995]
C. wrairi	Small intestine	[Vetterling, J.M. et al.,1971]

* Has been shown to cause human cryptosporidiosis

The *Cryptosporidium* apical complex is made up of several organelles; a single rhoptry, multiple micronemes and dense granules. These organelles are extruded from the apical end of the sporozoite and their secretions enhance gliding motility and attachment, and are critical for invasion of host cells (Chen, 2004, Bonnin, et al., 1993, Petersen, et al., 1992, Tomely and Soldadi, 2001). There are large numbers of micronemes present in
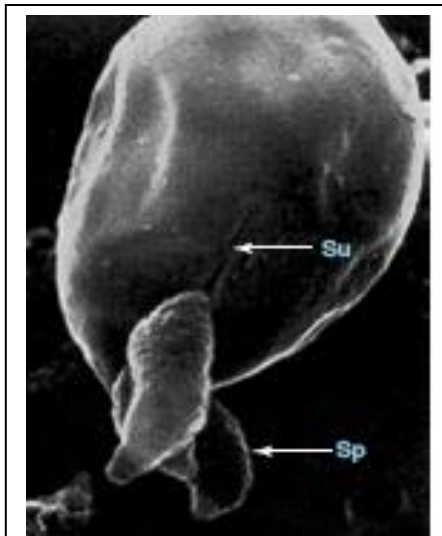
Figure 3. *Cryptosporidium* **sporozoites excysting from an oocyst.** The oocyst opens along a suture line (Su) releasing sporozoites (Sp) that may infect nearby epithelial cells (Smith, et al., 2005).

sporozoites. Micronemes are rod-like in appearance and excrete several proteins that function in gliding motility and attachment. These include thrombospondin related adhesive protein (TRAP-C1), as well as a number of glycoproteins (Langer and Riggs, 1999, Riggs, et al., 1999, Barnes, et al., 199, Ward and Cevallos, 1998). C. parvum possesses a single rhoptry, which is membrane-bound and plays a role in transforming the attachment site into the parasitophorous vacuole (Chen, Et al., 2004, Smith, 2005, Boulter-Bitzer, Et al., 2007). Dense granules remain distributed throughout the organism, and their function has not been fully elucidated. It has been proposed that they enable exchange between the Cryptosporidium parasite and the host cell and modify the host cell (Blackman and Bannister, 2001). In other apicomplexans, the function of dense granules is at least partially related to protein transport and formation of the parasitophorous vacuole (Cesbron-Delauw, 1994, Carruthers, Sibley, 1997).

Host cell invasion

Upon attachment to the host cell, the host cell membrane envelops the sporozoite into an intracellular, but extracytoplasmic, parasitophorous vacuole (Figure 4). The signals that trigger the formation of this vacuole are not known, although it appears that contact with the extruded rhoptry triggers morphologic changes in the host cell membrane character, causing the microvilli to become less apparent and the surface of the cell to smooth out and begin to extend around the attached zoite (Valigurová, A., et al., 2008). The parasite apparently causes sphingolipic-enriched membrane microdomains (SEM) in the host cell membrane to congregate. It activates enzymes involved in creating aggregation of these SEMs and this is tied to the remodeling of the host cell membrane. Actin remodeling within the host cell necessary for formation of the parasitophorous vacuole also seems to be tied to this activity (Nelson, et al., 2006). Another host cell function that is hijacked by *Cryptosporidium* is the control of water influx at the site of infection. The parasite triggers the host cell to increase the amount of water within the membrane, and this facilitates the protrusion of the host cell membrane around the parasite (Chen, et al., 2005).This is unusual among coccidians, as most form their own parasitophorous vacuoles without engaging host resources (Sibley, 2004). The micronemes become more organized longitudinally in the organism, and appear to form the pellicle for attachment. The position of the *Cryptosporidium* parasite is termed "epicellular" as it never comes into direct contact with the cytoplasm, remaining outside of the host cell membrane (Valigurová, A., et al., 2008). A feeder organelle, ostensibly a nutrient transport conduit from the host cell, has been observed (Figure 1).

Asexual reproduction: Type I merogony

When the parasitophorous vacuole is fully developed with the parasite within, it is referred to as a meront. The parasite within the meront, now referred to as a trophozoite,

11

undergoes asexual division, resulting in the development meront. Merozoites are

structurally similar to sporozoites (Fayer, et al., 2008). Type I of 4-8 merozoites within

the meronts are the first type formed and contain 6-8 merozoites. When the merozoites

have matured, the host cell membrane ruptures and they escape the meront and infect

more host cells, continuing the infection.

Asexual reproduction: Type II merogony

Following a number of cycles of merogony, a different type of meront, a Type II

meront, is formed. The merozoites from Type II meronts are believed to develop into

either microgamete (male), or macrogametes, (female). The trigger for development of

Type II meronts is not known for *Cryptosporidium*. Morphological differentiation

between types I and II meronts is based on the number of merozoites within each.

Although researchers have not yet found differentiating markers for Type I and II meronts,

there is some evidence of variance in the production of certain replication enzymes that
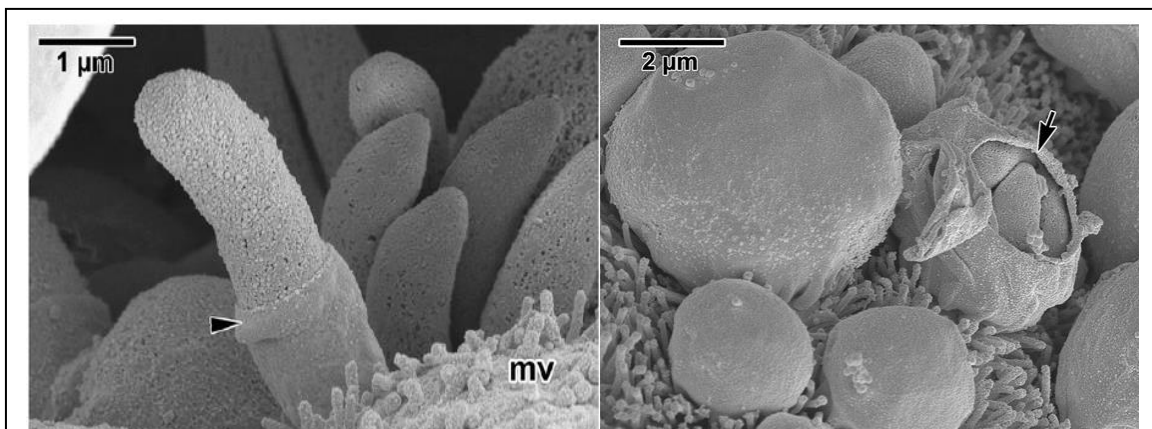
Figure 4. Attachment of sporozoites and formation of tropozoites. A. An electron micrograph shows a sporozoite being enveloped by host cell membrane (arrowhead). The host membrane can been seen advancing along the sporozoite, tightly enveloping it. The microvilli (mv) of host epithelial cells are visible near parasites. B. Developmental stages of *Cryptosporidium*. Trophozoites mature into merozoites within parasitophorous vacuole. A ruptured merozoite (arrow) reveals merozoites within (Valigurová, A., et al., 2008).

may provide the ability to positively identify the two different types of meront (Rider and Zhu, 2008).

Sexual reproduction: Gametogony

Sexual reproduction, or gametogony, is initiated when host cells are infected with merozoites that develop into microgamonts and macrogamonts, rather than meronts (Current and Reese, 1986).

Microgamonts are multinucleate and develop up to sixteen microgametes while macrogamonts contain only one nucleus. Microgametes, which are released and attach to the host cells containing macrogamonts, penetrate and fertilize the macrogamonts (Current and Reese, 1986). Upon fertilization, a zygote is formed. This develops into a sporulated oocyst containing four sporozoites (Fayer, et al., 2008, Thompson, et al., 2005). Both thin-walled and thick-walled oocysts are produced and are released from the host cell membrane. Thin-walled oocysts reinfect the current host, and thick-walled oocysts are the form observed in the environment. They are shed in the feces and may continue the infectious cycle in another host.

Advantageous characteristics

Cryptosporidium species have unique characteristics that allow their persistence in a wide variety of environments. A robust environmental life stage, low infectious dose, and a complex life cycle that can be carried out in a single host synergize with the intracellular, extracytoplasmic position within the infected host cell to provide advantages to the persistence and propagation of the Cryptosporidium parasite.

The infectious dose (ID_{50}) of *C. parvum* has been experimentally determined to be as low as 132 oocysts in healthy human subjects (DuPont, et al., 2005). In *C. hominis* infections, the ID_{50} may be as low as 10 oocysts (Chappell, et al., 2006). This low

infectious dose can explain why contamination of recreational water supplies can cause outbreaks. A single swimmer shedding oocysts is able to shed enough oocysts to infect numerous people. The low ID_{50} also means that a large volume of water is not needed to infect someone; a swallowed mouthful of water could contain enough oocysts to cause an infection.

Cryptosporidium is monoxenous, which is advantageous in that the complete life cycle can be carried out once an infection is established, rather than needing transfer from one host to another. This is more typical of the Gregarines than the Coccidians, as most coccidians carry out their life cycle in multiple hosts, rather than monoxenously (Kopecná, et al., 2006).

Cryptosporidium exploits a distinctive mechanism of parasitism within the host cell that is not shared by any other known parasite. It exists in an epicellular location outside of the host cytoplasm in a parasitophorous vacuole within the host cell membrane. As the parasite is covered by the host's membrane, it escapes direct detection by antibodies or immune cells, as an extracellular parasite would be. Secondly, by avoiding contact with the cytoplasm, *Cryptosporidium* avoids detection via presentation through the MCH Class I pathway as an intracellular parasite would be. In addition to its placement in an immunologically protected niche, this mechanism may allow *Cryptosporidium* parasites to share the host pool with other parasites without direct competition.

Oocyst structure

The structure of the oocyst wall has at least three distinct layers. The outer layer is made up of glycoproteins (Reduker, et al., 1985a; Harris and Petry, 1999). The rigid middle layer, made up of complex lipids, is responsible for the acid-fast nature of the

Figure 5. Suggested thick-walled oocyst wall structure. Four distinct layers provide strength and resistance to environmental influences, and from chemical treatments (Jenkins, et al., 2010).
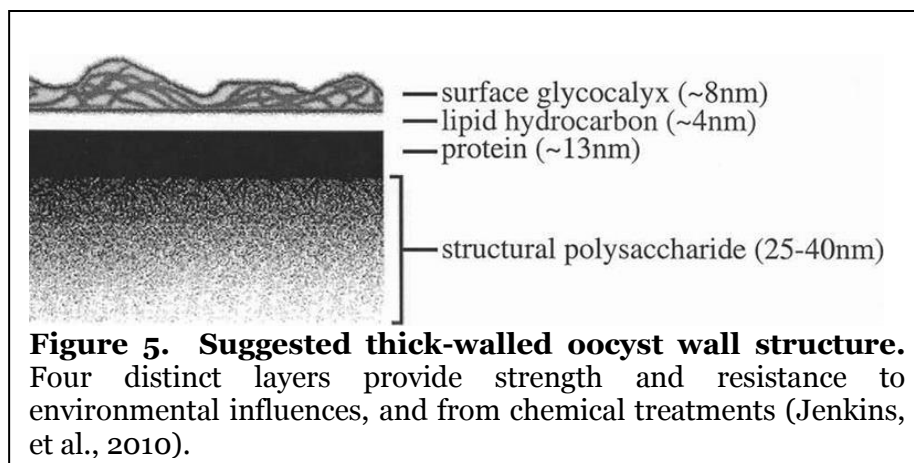
organism. And the thick inner layer is made up of filamentous glycoprotein lipid (Bonnin, et al., 1991) . Recently, a more detailed organizational structure has been proposed (Fig. 5, Jenkins, et al., 2010). This model shows four layers; the glycocalyx, a lipid layer, a high-protein layer, and an inner polysaccharide layer.

Due to the complex life cycle of the organism the formation of an oocyst has not been directly observed, but a number of the molecules that make up the oocyst have been identified. The *Cryptosporidium* oocyst wall protein (COWP) family of 8 proteins is unique to the *Cryptosporidium* species, but homologs have been detected in *Toxoplasma* species, suggesting that the COWP proteins play a structural role in environmental survival of cysts (Templeton, et al., 2004). Using monoclonal antibodies (Ab), COWP1 and COWP8 have been localized to the inner layer of the oocyst wall. These proteins are useful for identification of the oocyst stage and may provide drug targets for treatment. Unique glycoproteins that are thought to tether sporozoites to the oocyst wall in *C. parvum* (Chatterjee, et al., 2010) may also provide potential targets for identification.

Thin-walled oocysts contain four sporozoites, just as the thick-walled oocysts do, but they are only covered with a membrane. Lacking the thick, multi-layered wall of thick-walled oocysts, they are too fragile to survive shedding and environmental stresses (Fayer,

et al., 2008). Thin-walled oocysts excyst while still within the host intestine, continuing the autoinfectous cycle until the host's immune system clears the infection.

With both sexual and asexual stages, the *Cryptosporidium* life cycle allows a rapid increase in parasite numbers within the host, reinfection of the same host, and efficient transport of infectious forms to new hosts. Multiple members of the phylum Apicomplexa have both sexual and asexual reproductive stages, and in some species, the triggers that cause the switch to sexual stages have been defined. For example, the coccidian *Eimeria tenella* is genetically preprogrammed to switch to gametogeny after two generations (McDougald and Jeffers, 1979). However, it is not known what the trigger for gametogony is in *Cryptosporidium* species.

Life cycle terminology

Apicomplexans, in general, replicate by both asexual and sexual processes; all are parasites; and all possess the characteristic apical complex in their infectious stage, which defines their classification. The stages of the life cycle consist of asexual merogony, sexual gamogony, and sporogony in which infectious cysts are formed (Levine, 1988). The life cycle of *Cryptosporidium* is similar to those of other members of the Apicomplexa. However, the vocabulary of the Apicomplexa group is complicated by similar stages and similar cycles that are sometimes referred to by different names.

In *Cryptosporidium*, the infecting oocyst contains four mature sporozoites, which escape the oocyst during excystation to invade host cells. Once a sporozoite or merozoite is completely enveloped in the host membrane, it rounds up and becomes a trophozoite. The trophozoite is an asexually-reproducing feeding form. The trophozoite undergoes asexual reproduction (merogony), producing daughter merozoites. When merozoites are produced, the intracellular organism is now a meront. The mature meront bursts and the merozoites infect new cells, becoming trophozoites and starting the cycle anew.

Transmission: Route of infection

Cryptosporidium is transmitted by a fecal-oral route. Human-to-human transmission can be through contact with an infected person's feces or through contact with contaminated surfaces, drinking water, recreational water, or food sources. Improper hand washing and diaper changing practices can expose people to oocysts (Fayer, et al., 2000). Water-borne infections and outbreaks were first noted in 1984. Oocysts can be found in drinking water, due to fecal contamination of water sources and failures in water treatment. Rivers and lakes can become contaminated by run-off containing the feces of infected animals. Recreational water sources are now being recognized as a common source of oocysts and even the chlorine treatment of residential swimming pools will not kill the hardy thick-walled oocyst. (Fayer, et al., 2000, Casman, 2000).

Zoonotic transmission can occur in several ways. *C. parvum* is the most common zoonotic species, but several other species of *Cryptosporidium* have been detected in human outbreaks (see Table 3). Fecal contamination of water sources by infected cattle or other domesticated animals can affect bodies of water used by humans who may drink or swallow the contaminated water and become ill. People working around infected farm animals can also contract cryptosporidiosis by coming into direct contact with the animal feces (Fayer, et al., 2000, Xiao, et al., 2004). Although *Cryptosporidium* has been detected on fresh produce, most likely due to rinsing with contaminated water, it is unknown how many people have actually contracted cryptosporidiosis in this way (Yoder, et al., 2010). A 2012 outbreak in England and Scotland that sickened 300 people was linked to pre-washed salad mix (Health Protection Agency, 2013).

Cryptosporidiosis

Human cryptosporidiosis is characterized by severe, watery diarrhea, often with stomach cramps and low-grade fever. Patients may also suffer from a loss of appetite,

nausea, and vomiting (Yoder, et al., 2010). Cryptosporidiosis is self-limiting in immunocompetent individuals. However, when immunocompromised individuals are infected, chronic diarrhea can result in life-threatening dehydration. Until the AIDS epidemic introduced cryptosporidiosis as a potentially life-threatening condition, definitive diagnoses were not routinely made. AIDS patients, immunosuppressed patients, very young or very old patients, as well as those suffering from poor nutrition are at increased risk of severe disease or death from cryptosporidiosis (Hunter and Nichols, 2002).

Course of disease in the immunocompetent host

Acute human cryptosporidiosis is characterized by severe, watery diarrhea and stomach cramps. Contributing symptoms may include low-grade fever, nausea, anorexia, and vomiting (Yoder, et al., 2010). There is some evidence that symptoms are dependent upon the infecting species. *C. homins* infections are more frequently associated with severe symptoms (Cama, et al., 2008, Gatei, et al., 2006). After oocysts are ingested, there is an incubation period of 2 - 7 days before symptoms appear (Ramierez, et al., 2004, Jokipii and Jokipii, 1986). Acute clinical symptoms can last as few as 2 days or as many as 120 days. The average duration of symptoms is one to three weeks (Jokipii and Jokipii, 1986, MacKenzie et al., 1995, Robertson, et al., 2002). Oocyst shedding typically is detected a couple days following the onset of symptoms (Chappell, et al., 2006). Although shedding (patent period) typically lasts only a week or two, cases of healthy patients shedding oocysts for up to several months after their symptoms have stopped have been documented (Yoder, et al., 2010, Fayer, 2004).

Sporadic recurrence of cryptosporidiosis within individuals is documented in many cases. Some research groups have estimated 30-40% of infected patients have recurrent

infections. When species identification has been carried out, *C. hominis* is the most

frequently detected in recurrent cases (MacKenzie, et al., 1995, Hunter, et al., 2004b).

Course of disease in the immunocompromised host

Immunocompromised patients, whether suffering from HIV/AIDS, undergoing

chemotherapy, or impacted by other forms of decreased immune function, are not able to

clear a *Cryptosporidium* infection. The chronic diarrhea can quickly lead to dehydration

and, in severe cases, death (Hunter and Nichols, 2002). In addition, HIV/AIDS patients

are more likely to become chronically infected with *Cryptosporidium* and to experience

extra-intestinal atypical infections. *Cryptosporidium* infections have been observed

throughout the gastrointestinal tract, in the gall bladder, pancreatic duct, the respiratory

system, and the biliary tree of HIV/AIDS patients (Chen, et al., 2002, Baishanbo et al.,

2006). The severity of cryptosporidiosis in the context of severe immunodeficiency seems

to be directly related to the CD4$^+$ T-cell count. Patients with CD4$^+$ T-cell counts

>200/mm^3 have no more severe symptoms than immunocompetent patients, while AIDS

patients with CD4$^+$ T-cell counts <50/mm^3 tend to have chronic, severe symptoms with

high mortality rates (Hunter and Nichols, 2002).

Hunter and Nichols also reported on cryptosporidiosis in immunocompromised

individuals who did not have HIV/AIDS. The disease is not nearly as prevalent in this

population as with HIV/AIDS. Although often contradictory, general findings show that

only immunodeficiencies causing T-cell deficiencies are likely to cause more severe

symptoms if the patient contracts cryptosporidiosis (Hunter and Nichols, 2002).

Pathology of cryptosporidiosis

The pathology of cryptosporidiosis on the human intestine involves physical

changes to the intestinal lumen, increased porosity and secretory action of the intestines,

damage to host cells, and loss of fluids (Chen and LaRusso, 1999). In immunocompetent individuals, epithelial changes are observable by endoscopy and biopsy. These include a loss of the microvillous nature of the intestinal epithelial cells and a blunting of the villi. In addition to blunting, other changes to the villi that have been observed include atrophy and hyperplasia of crypt cells. Furthermore, the lamina propria shows evidence of an influx of immune cells (Meisel, et al., 1976; Farthing, 2000).

Changes in intestinal electrolyte concentrations may be responsible for the influx of fluids, which cause the watery stools associated with cryptosporidiosis. A combination of decreased sodium absorption and increased chloride secretion due to changes in epithelial cells creates a hypertonic environment, which causes a net flow of fluids into the intestines (Argenzio et al., 1990). In addition to increased fluids, the disruption of epithelial integrity reduces absorption of fluids, increasing the effect (Adams et al., 1994; Griffiths et al., 1994). Colonoscopy or biopsies from HIV/AIDS patients show intestinal epithelial tissue damage that is evident at a much larger degree than in that of immunocompetent patients. It is believed that the lack of intraepithelial lymphocytes enables the parasite to damage the tissue without challenge (Hunter and Nichols, 2002).

Cryptosporidium has also been shown to exhibit some control over host cell apoptotic pathways. Early in the infection, apoptosis is inhibited. The mechanism is not understood, but host pro-apoptosis genes are down regulated during initial stages of infection. Later, when meronts are mature and merozoites need to escape the host cell, pro-apoptotic genes are up regulated, killing the cell and freeing the parasites from the host cell (Liu, et al., 2008, Liu, et al., 2009, Platner and Soldati-Favre, 2008).

Host immune response

Although the precise mechanism by which the immune response eliminates the infection is not well understood, the host does eventually clear the *Cryptosporidium*

parasite. Adult murine models have shown that early in the infection interferon gamma (IFN-γ) production by intraepithelial CD8+ cells in the host intestine increases (Barakat, 2009, Leav, 2005). This cytokine is believed to be important in a protective host response since a *C. parvum* infection may be established in IFN-γ knockout mice while those with normal or exogenously supplemented IFN-γ quickly clear the parasite (Leav, 2005).

In humans, T cell-mediated immunity appears to play an important role in eliminating *Cryptosporidium* and protecting intestinal epithelial cells from damage (Leav, 2005). In personnias with HIV/AIDS, disease severity and chronicity varies inversely with the number of CD4+ lymphocytes in the patient's blood. This is not clearly understood, but it would seem that CD4+ cells play an important role in triggering release of IFN-γ (Hunter and Nichols, 2002).

Recovery from cryptosporidiosis is believed to confer at least a low level of immunity to the infecting species. The fact that young children are far more likely to develop clinical disease suggests that exposure earlier in life provides some resistance to infection later (Chalmers and Davies, 2010).

Current treatment and chemotherapy options

Finding an effective treatment for the prevention or cure of cryptosporidiosis has proven elusive. *Cryptosporidium* species have not responded to drugs that are effective against other coccidian parasites (Thompson, et al., 2005). Various antibacterial drugs have been tested against *Cryptosporidium in vitro,* and a there have been a few clinical trials in humans, but only two drugs have been tested in-depth as anti-*Cryptosporidial* treatments (Rossignol, 2010). Paromomycin, an aminoglycoside that targets ribosomes, showed initial promise in reducing the number of episodes of diarrhea and the number of oocysts shed in AIDS patients. Subsequent testing showed mixed results, and

Paromomycin is not regularly used to treat cryptosporidiosis (Rossignol, 2010, Hewitt, et al., 2000, Theodos, et al., 1998, Fichtenbaum, et al., 1993).

Nitazoxanide is currently the only drug routinely used to treat cryptosporidiosis. Since several aromatic dicationic molecules have shown anti-parasitic potential, a study was done testing them for efficacy against *Cryptosporidium parvum* in particular. Of the compounds tested, nitazosanide and paromomycin showed promise for reducing the number of parasites in the infected mice (Blagburn, et al., 1998). Full-scale clinical trials were carried out, and although it did not improve the outcome for HIV/AIDS patients, nitazoxanide was approved for use in non-immunosuppressed children and adults (Rossignol, 2010). The mechanism of action appears to be interference with the pyruvate:ferredoxin oxidoreductase (PFOR) enzyme-dependent electron transfer reaction, which is necessary for *Cryptosporidium* metabolism (Amadi, et al., 2002, Giles and Hoffam, 2002). As stated earlier, it appears that the most effective treatment for cryptosporidiosis in immunocompromised patients is treatments to partially restore immune function, such as HAART (Amadi, et al., 2002, Gomez-Morales, 2004).

Potential treatments for cryptosporidiosis

A recent study tested 39 derivatives of nitazoxanide against nitazoxanide for effectiveness. Substitutions were made for the nitro group on the thiazole ring and/or for one or more of the R groups on the benzene ring. Some of the new compounds show higher levels of action against *Cryptosporidium* than nitazoxanide, particularly those with halogens substituted for the nitro group (Gargala, et al., 2010). While promising, these drugs are in the early phases of testing, so it will be years before they would be feasible clinical treatments.

Recently, a research group investigating drugs that target an apicomplexan topoisomerase similar to bacterial topoisomerases has found that antibiotics will target

Apicomplexans in addition to bacterial species. However, *Cryptosporidium* is not affected by this mechanism of antibiotic action as it lacks an apicoplast organelle (García-Estrada, et al., 2010). This demonstrates once again the difficulty of finding suitable drug targets for *Cryptosporidium*.

Vaccination has not yet been effective for cryptosporidiosis prevention, although recent work in an animal model using a DNA vaccine encoding for *C. parvum* surface proteins Cp12 and Cp21 has showed excellent results in early testing. These antigens are the dominant immunogens in the immune response to *C. parvum*. In the study, vaccinated mice produced anti-*C. parvum* Ab and also resisted infection when challenged with *C. parvum* (Yu, et al., 2010). It will remain to be seen if this protective effect will be reproducible in humans or if the vaccine is cross-protective for other *Cryptosporidium* species. In addition, another surface protein, Cp15, which is immunodominant has shown some promise as a vaccinogen. A successful vaccination program would be significant, especially in developing countries with poor health care and limited access to treatment (Manque, et al., 2011). Barriers to an effective vaccination program, if such a vaccine is developed, would include the high cost of vaccination programs and vaccination would not eliminate malnourishment, which can also reduce immunocompetency.

Epidemiology: Surveillance and outbreaks

Since cryptosporidiosis was first classified as a reportable condition in 1995, the number of U.S. cases has increased from a low of 2,426 in 1996 to a high of 11,657 cases in 2007 (Montelbano, et al., 1997, Yoder, et al., 2010). This is likely an underestimation, as testing isn't common unless there is a concern that the patient's immune system is compromised. The CDC has recently reviewed the criteria for reporting cryptosporidiosis. This will probably decrease the number of cases reported, as a case must now exhibit both the defined symptoms of the disease and be identified as *Cryptosporidium* by positive

laboratory testing to be reported. Previously, positive lab identification, even in asymptomatic individuals was reportable (Yoder, et al., 2010).

Outbreaks of cryptosporidiosis are more frequent in summer months, due to increased participation in water recreation activities at municipal pools, water parks, and swimming areas. Oocysts entering the water from a single infected person may infect many others.   Since many of the mechanisms that control pathogens are not effective in eliminating the robust, chlorine-tolerant oocyst, municipal water systems are at risk for *Cryptosporidium* contamination and have the potential to infect large numbers of citizens. Cryptosporidiosis has the potential to have economic and social impact, in addition to health concerns, even among immunocompetent people. When recreational water sources can become contaminated, and many people are affected at one time, there is going to be impact on multiple levels. There are a number of outbreaks already documented.

Milwaukee outbreak

In the spring of 1993, over the course of two months, an epidemic of watery diarrhea plagued Milwaukee, Wisconsin. Laboratory tests confirmed many cases of cryptosporidiosis. Using statistical methods and telephone polling, the number of *Cryptosporidium* cases was estimated to be as high as 403,000 (MacKenzie, et al., 1995). Estimates range from 50-100 fatalities related to this outbreak (Hoxie, et al., 1997). Although the cause of the outbreak was not identified, increased turbidity in one of the city's water plants was noted in the weeks preceding the outbreak and some of the water plant's filters had been incorrectly installed. It was assumed that oocysts had passed through the water treatment plants and to many of the residents of that city, resulting in the largest cryptosporidiosis outbreak ever recorded. This outbreak illustrated deficiencies in current policies and spurred changes in treatment and monitoring of water treatment

(Zhou, et al., 2003). Since 1993, water purification and treatment plans have been revised to improve removal of oocysts and increase monitoring for the parasite.

England outbreak: Rabbit genotype

An outbreak in England in 2008 was traced to infection of the municipal water supply in Northamptonshire, England when a rabbit infected with *Cryptosporidium* sp. rabbit genotype died in a remote ancillary water tank in the reservoir that supplied 250,000 residents ("Sickness bug found," 2008). Thirty-four laboratory-identified cases of cryptosporidiosis were checked for genetic homology to the parasite isolated from the dead rabbit. Of these, a majority (23) matched the newly identified rabbit genotype (Chalmers, et al., 2009). The other samples were either not able to be typed or were genotypes other than rabbit. This was unusual because the rabbit genotype is not typically considered pathogenic to humans. Despite a notice for citizens to boil their water, more than two dozen cases of cryptosporidiosis were reported ("Sickness bug found, 2008).

Outbreak among firefighters in Indiana and Michigan

An unusual outbreak occurred in June of 2011 when 20 firefighters reported cryptosporidiosis following a response to a barn fire. The barn housed 240 week-old calves, many of which were infected with *C. parvum*. In addition, a swimming pond nearby that was used as a water source to extinguish the fire was also contaminated with *C. parvum*. Disease surveillance revealed that fire fighters who had direct contact with calves (carrying or leading them from the barn), who washed themselves in water from the swimming pond, or who drank water from a cooler of with an unidentified source were more likely to have gastrointestinal disease (Wilczynski, et al., 2012).

Water treatments to remove *Cryptosporidium* oocysts

In addition to surviving environmental stresses, the oocysts are also highly resistant to chemical treatment. The current chlorine treatment commonly used to kill bacteria and viruses in municipal water systems does not kill the *Cryptosporidium* oocysts (Fayer, et al., 2000, Casman, 2000). Municipal water treatment plants must remove particulate material from source water to prevent the *Cryptosporidium* oocysts from contaminating drinking water. Typical water treatment removes *Cryptosporidium* during two stages. First, source water is allowed to stand in reservoirs for several weeks allowing much of the particulate matter, including oocysts, to settle to the bottom, which will die after several weeks (MacKenzie, et al., 1994). Coagulation using agents that encourage particles to clump together, followed by flocculation, which stirs water, increasing coagulation, also removes *Cryptosporidium* oocysts. Filtration further removes any remaining oocysts. Other mechanisms to eliminate oocysts are being trialed, such as UV light treatment, and are showing some promise for eliminating *Cryptosporidium* sp. from water supplies (Betancourt and Rose, 2004).

Research challenges

Research on *Cryptosporidium* began in earnest when it became recognized as a pathogen of economic concern for cattle ranchers, as it can dramatically affect calf weight, and that it could cause severe disease in immunocompromised humans (Thompson, 2008). Research includes a focus on many aspects of cryptosporidiosis, including epidemiology, pathology, immunology, and chemotherapy, as well as understanding the life cycle, species identification, and host-specificity of *Cryptosporidium* sp.

Laboratory studies of *Cryptosporidium* are challenging due to the complex life cycle of the organism. *C. parvum*, the zoonotic species that infects humans, does not infect small laboratory model animals such as rats or mice unless they are

immunocompromised. An infection with *C. parvum* can be initiated in neonatal mice less than three weeks of age, but these infections produce few oocysts. After about three weeks, the murine immune system matures and is resistant to infection by *C. parvum.* Additionally, neonatal mice are difficult to work with due to their small size. *C. parvum* does infect cattle, and this host is used to propagate oocysts. However, the cost, maintenance, and size of these animals limit their use in many experimental situations.

Available *Cryptosporidium* isolates

Isolates of *Cryptosporidium* species are available from a limited number of sources. Oocysts can be obtained from laboratories that either amplify the parasite in calves or in immunocompromised mice. Due to these limited options for *in vivo* propagation, maintaining a large number of different *Cryptosporidium* species for research is not practical. The American Type Culture Collection (ATCC) currently has seven strains of *Cryptosporidium* available for use. These are listed in table 4 along with the depositors of each strain.

Culturing techniques and limitations

Cell culture techniques have been employed for growing and studying *Cryptosporidium in vitro.* Three of the most often used cell lines include human colonic adenocarcinoma (Caco-2), human colonic tumor (HCT-8), and Madin Darby canine kidney (MDCK). These cell lines will support a *Cryptosporidium* infection through oocyst production (Arrowood, 2002).

A standard method for growing *C. parvum in vitro* is to infect a nearly-confluent monolayer of mammalian cells with oocysts and then incubate this cell culture in medium containing up to 10% serum at 37ºC under 5% CO_2. An infection may progress for up to several days. *In vitro* infections allow both sexual and asexual stages to be observed. All

Table 4. American Type Culture Collection (ATCC) *Cryptosporidium* strains

ATCC number	Species	Designation (Isolate)	Depositors
87664	*Cryptosporidium serpentis*	KSU-2	SJ Upton, NV Khramtsov
87666	*Cryptosporidium muris*	108735	SJ Upton, NV Khramtsov
87668	*Cryptosporidium parvum*	IowaI	SJ Upton, NV Khramtsov
87712	*Cryptosporidium parvum*	UCP	SJ Upton, NV Khramtsov
87715	*Cryptosporidium sp.*	VS1742 Idaho-1	SJ Upton, NV Khramtsov
87763	*Cryptosporidium parvum*	Galicia	NV Khramtsov, SJ Upton
87765	*Cryptosporidium parvum*	Columbia	NV Khramtsov, SJ Upton

life stages of *C. parvum* can be observed using cell culture techniques; however, culture conditions limit the duration of the active infection. Maintaining the infection is possible only as long as the host cell monolayer is viable. Host cell death in the monolayer and a lack of access to new host cells for infection contribute to the difficulty in successfully maintaining a long-term *in vitro* infection (Arrowood, 2002). Multiple techniques have been used to attempt to slow host cell growth, and hence, overcrowding of the monolayer and cell death. These include lightly irradiating the host cells prior to infection and limiting the amount of serum available in the culture medium. This has extended the length of infections up to two weeks (Hijjawi, 2010).

A method utilizing a micro-gravity environment and a rotating cell-culture system has been developed to study *Cryptosporidium* infections. Using observations of three-dimensional cell culture growth on the Space Shuttle, cell culture using an apparatus to create a situation that will keep cells in suspension results in development of what has been coined "organoid" growth (Hammond, et al., 2000). Cells begin to differentiate and more closely resemble an intestine than a monolayer of cells. Pseudo-villi develop with fringed border cells. This provides a more realistic model of *Cryptosporidium* pathology

than traditional cell culture (Warren, et al., 2008). This could be significant for *Cryptosporidium* research as it much more closely replicates the normal environment for *Cryptosporidium* infections, and could provide a better look at the effect on host cells and the behavior of the parasite.

Understanding and identifying life stages

Microscopic examination of stained *Cryptosporidium* infections can be used to determine the life stage the parasite. Staining and identification of structural differences using differential interference contrast (DIC) microscopy can aid in identifying various life stages. Type I meronts contain 6-8 merozoites while Type II meronts contain only four. Figure 6 illustrates that differentiation of these stages can be accomplished with fluorescence (A) or DIC microscopy (B).

Figure 6. Type I and Type II meronts.
 (A) A photomicrograph of a Type 1 meront bearing six fluorescently stained merozoites (yellow).
(B) A photomicroph of a Type II meronts utilizing Differential Interference Contrast microscopy to differentiate four distinct merozoites within the meronts.
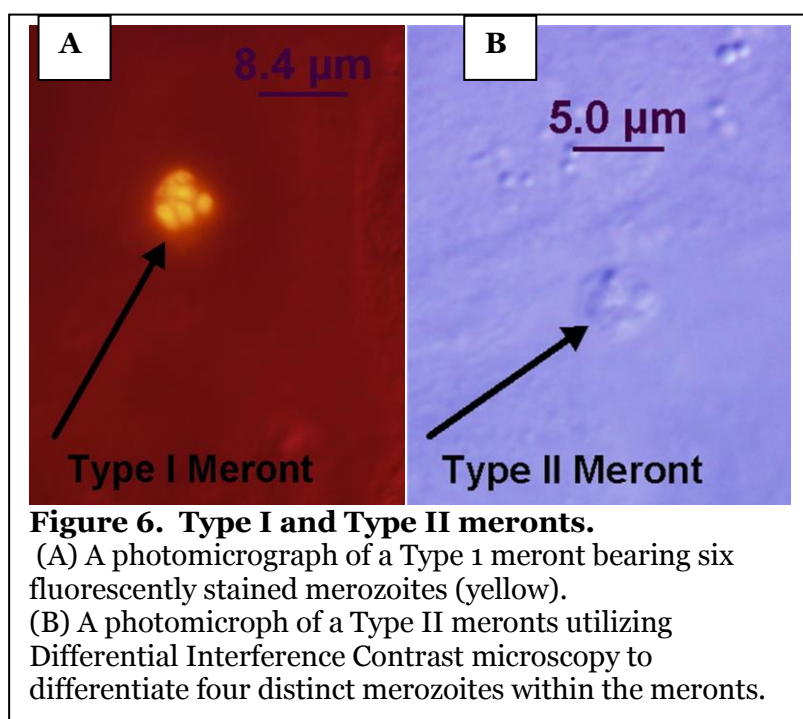
Commercial rapid stain kits are available to aid in identification. Sporo-Glo ™ from Waterborne, Inc. uses polyclonal, fluorescein-labeled rat anti- *Cryptosporidium*

parvum antibodies to label intracellular stages. Sporozoites and merozoites can be labeled to fluoresce green under fluorescent microscopy. Waterborne's Crypt-a-Glo™ uses mouse anti-oocyst monoclonal antibodies labeled with fluorescein to label *Cryptosporidium* oocysts

Immunohistochemical staining of *Cryptosporidium* is also used for microscopic study. A variety of monoclonal and polyclonal antibodies are available.

Currently, there are no staining methods that can differentiate between Type I and Type II meronts. Antibodies are able to detect either intracellular stages, or oocyst structure, but differentiating between Type I and Type II meronts remains subjective. Some lectins have been shown to bind to certain glycoproteins on *Cryptosporidium* cells and oocysts. Using labeled lectins to stain infected monolayers of host cells can allow the *Cryptosporidium* cells to be visualized either with fluorescent or chromogenic stains.

Genetic analysis

PCR analysis can be used to determine genetic expression at various stages of an infection. Actively growing and dividing cells express *18S* rRNA, which has been used as a baseline RNA level to monitor the development of the infection using real-time PCR. Traditionally, a declining level of *18S* has been used as a marker of a failed or nonproductive infection. Some of the genes that have been used for study include *COWP1 - 9, TRAP, and HSP70.* (Templeton and Kaslow, 1997; Robson et al., 1998; Spano, et al., 1997).

Objectives of the project

The long-term objective of this research project is to understand the role of host-pathogen adaptations in health and disease. A critical aspect of this research is the development of standardized laboratory techniques that can be used to examine changes

in *Cryptosporidium* infection. This research project represents a first step in determining the critical aspects of *Cryptosporidium* infection that signal the vitally important switch from asexual to sexual life cycle stages that indicate the production of infectious organisms. The central hypothesis of this work is that the switch from an asexual to a sexual stage is a function of the availability of host cells to infect rather than a time-dependent switch.

References

Adams, R.B., Guerrant, R.L., Zu, S., Fang, G., Roche, J.K., 1994.
Cryptosporidium parvum infection of intestinal epithelium: morphologic and functional studies in an *in vitro* model. J. Infect. Dis. **169**, 170–177.

Alvarez-Pellitero, P., Sitjà-Bobadilla, A., 2002. *Cryptosporidium molnari* n. sp. (Apicomplexa: Cryptosporidiidae) infecting two marine fish species, *Sparus aurata* L. and *Dicentrarchus labrax* L.. Int. J. Parasitol. **32**, 1007–1021.

Amadi, B., Mwiya, M., Musuku, J., Watuka, A., Sianongo, S., Ayoub, A., Kelly, P., 2002. Effect of nitazoxanide on morbidity and mortality in Zambian children with cryptosporidiosis: a randomized control-led trail. Lancet **360**, 1375-1380.

Argenzio, R.A., Laicos, J.A., Levy, M.L., Meuten, D.J., Lecce, J.G., Powell, D.W., 1990. Villous atrophy, crypt hyperplasia, cellular infiltration and impaired glucose-Na absorption in enteric cryptosporidiosis of pigs. Gastroenterol. **98**, 1129–1140.

Arrowood, M., 2002. *In vitro* Cultivation of *Cryptosporidium* Species. Clin Microbiol Rev. **15,** 390-400.

Baishanbo, A., Gargala, G., Duclos, C., François, A., Rossignol, J.F., Ballet, J.J., Favennec, L., 2006. Efficacy of nitazoxanide and paromomycin in biliary tract cryptosporidiosis in an immunosuppressed gerbil model. J. Antimicrob. Chemother. **57**, 353–355.

Ballard T. E., Wang X., Olekhnovich I., Koerner T., Seymour C., Hoffman P. S., Macdonald T. L., 2010. Biological activity of modified and exchanged 2-amino-5-nitrothiazole amide analogues of nitazoxanide. Bioorg. Med. Chem. Lett. **20**, 3537-3539.

Barakat, F.M., McDonald, V., Foster, G.R., Tovey, M.G., Korbel, D.S., 2009. *Cryptosporidium parvum* infection rapidly induces a protective innate immune response involving type I interferon. J. Infect. Dis. **200,** 1548-1555.

Barnes, D.A. et al.,1998. A novel multi-domain mucin-like glycoprotein of *Cryptosporidium parvum* mediates invasion. Mol. Biochem. Parasitol. **96**, 93–110.

Blagburn, B. L., Drain K. L., Land, T. M., Kinard, R. G., Moore P. H., Lindsay D. S., Patrick D. A., Boykin D. W., Tidwell R. R., 1998. Comparative efficacy evaluation of dicationic carbazole compounds, nitazoxanide, and paromomycin against *Cryptosporidium parvum* infections in a neonatal mouse model. Antimicrob. Agents Chemother. **42**, 2877-2882.

Bonnin A, Dubremetz JF, Camerlynck P., 1993. A new antigen of *Cryptosporidium parvum* micronemes possessing epitopes cross-reactive with macrogamete granules. Parasitol. Res. **79**: 8–14.

Bonnin A., Dubremetz J. F., Camerlynck P., 1991. Characterization and immunolocalization of an oocyst wall antigen of *Cryptosporidium parvum* (Protozoa: Apicomplexa). Parasitol. **103** (2), 171-177.

Boulter-Bitzer J. I., Lee H., Trevors J. T., 2007. Molecular targets for detection and immunotherapy in *Cryptosporidium parvum*. Biotechnol. Adv. **25**:13-44.

Cama, V.A., Bern, C., Roberts, J., Cabrera, L., Sterling, C.R., Ortega, Y., Gilman, R.H., Xiao, L., 2008. *Cryptosporidium* species and subtypes and clinical manifestations in children, Peru. Emerg. Infect. Dis. **14**, 1567–1574.

Carreno, R.A., Martin, D.S., Barta, J.R., 1999. *Cryptosporidium* is more closely related to the gregarines than to coccidia as shown by phylogenetic analysis of apicomplexan parasites inferred using small-subunit ribosomal RNA gene sequences. Parasitol. Res. **85**, 899–904.

Carruthers, V.B., Sibley, L.D., 1997. Sequential protein secretion from three disctinct organelles of *Toxoplasma gondii* accompanies invasion of human fibroblasts. Eur. J. Cell Biol. **73**, 114–123.

Casemore, D.P., Armstrong, M., Sands, R.L., 1985. Laboratory Diagnosis of cryptosporidiosis. J. Clin. Pathol. **38**, 1337-1341.

Casman, E.A., Fischhoff, B., Palmgren, C., Small, M.J., Wu, F., 2000. An integrated risk mode of a drinking-water-borne Cryptosporidiosis outbreak. Risk Analy. **20**, 495-511.

Cesbron-Delauw, M.F., 1994. Dense granule organelles of *Toxoplasma gondii*: their role in the host–parasite relationship. Parasitol. Today **8**,293–296.

Chalmers, R.M., Davies, A.P., 2010. Minireview: clinical cryptosporidiosis. Exp Parasitol. **124**, 138-46.

Chalmers, R.M., Robinson, G., Elwin, K., Hadfield, S. J., Xiao, L., Ryan, U., Modha, D., Mallaghan, C., 2009. *Cryptosporidium* rabbit genotype, a newly identified human pathogen. Emerg. Infect. Dis. **15**, 829-830.

Chappell, C.L., Okhuysen, P.C., Langer-Curry, R., Widmer, G., Akiyoshi, D.E., Tanriverdi, S., Tzipori, S., 2006. *Cryptosporidium hominis*: experimental challenge of healthy adults. Am. J. Trop. Med. Hyg.**75**, 851–857.

Chatterjee A., Banerjee S., Steffen M., O'Connor R. M., Ward H. D., Robbins P. W., and Samuelson J., 2010. Evidence for mucin-like glycoproteins that tether sporozoites of *Cryptosporidium parvum* to the inner surface of the oocyst wall. Eukaryot. Cell. **9**, 84-96.

Chen, X.M., Gores, G.J., Paya, C.V., LaRusso, N.F., 1999. Cryptosporidium parvum induces apoptosis in biliary epithelia by a Fas/Fas ligand-dependent mechanism. Am. J. Physiol. **277**, 599–608.

Chen, X.M., LaRusso, N.F., 2002. Cryptosporidiosis and the pathogenesis of AIDS cholangiopathy. Semin. Liv. Dis. **22**, 277–289.

Chen X. M., O'Hara S. P., Huang B. Q., Nelson J. B., Lin J. J., Zhu G., Ward H. D., LaRusso N. F., 2004. Apical organelle discharge by *Cryptosporidium parvum* is temperature, cytoskeleton, and intracellular calcium dependent and required for host cell invasion. Infect Immun. **72**, 6806-6816.

Chen, X.M., O'Hara, S.P., Huang, B.Q., Splinter, P.L., Nelson, J.B., Larusso, N.F., 2005. Localized glucose and water influx facilitates Cryptosporidium parvum cellular invasion by means of modulation of host-cell membrane protrusion. Proc.Natl.Acad.Sci.U.S.A 102, 6338-6343.

Choudry, N., Bajaj-Elliot, M., McDonald, V., 2008. Terminal sialic acid of glycoconjugates on the surface of intestinal epithelial cells activates excystation of *Cryptosporidium parvum*. Infect. Immun. **76**, 3735-3741.

Current, W. L., L. S. Garcia., 1991. Cryptosporidiosis. Clin. Microbiol. Rev. **4**, 325-358.

Current, W. L., N. C. Reese, 1986. A comparison of endogenous development of three isolates of *Cryptosporidium* in suckling mice. J. Protozool. **33**:98–108.

Current, W.L., Upton, S., Haynes, T.B., 1986. The life cycle of *Cryptosporidium baileyi* n. sp. (Apicomplexa, Cryptosporidiidae) infecting chickens. J. Protozool. **33**, 289–296.

DuPont, H.L., Chappell, C.L., Sterling, C.R., Okhuysen, P.C., Rose, J.B., Jakubowski, W., 1995. The infectivity of *Cryptosporidium parvum* in healthy volunteers. N. Engl. J. Med. **332**, 855-859.

Farthing, M.J.G., 2000. Clinical aspects of human cryptosporidiosis. In: Petry, F. (Ed.), Cryptosporidiosis and Microsporidiosis. Contributions in Microbiology **6**. Karger, Basel, pp. 50–74.

Fayer, R., 2004. *Cryptosporidium*: a water-borne zoonotic parasite. Vet Parasitol. 126, 37-56

Fayer, R., 2008. General biology. In: Fayer, R., Xiao, L. (Eds.), *Cryptospsoridium* and Cryptosporidiosis. CRC Press, Boca Raton, 1–42.

Fayer, R., 2010. Taxonomy and species delimitation in *Cryptosporidium*. Exp. Parasitol., **124**, 90-97.

Fayer R., Morgan, U., Upton, S. J., 2000. Epidemiology of *Cryptosporidium*: transmission, detection and identification. Int. J. Parasitol. **30**, 1305-22.

Fayer, R., Santín, M., Trout, J.M., 2008. *Cryptosporidium ryanae* n. sp. (Apicomplexa: Cryptosporidiidae) in cattle (Bos taurus). Vet. Parasitol. **156**, 191–198.

Fayer, R., Santín, M., Xiao, L., 2005. *Cryptosporidium bovis* n. sp. (Apicomplexa: Cryptosporidiidae) in cattle (*Bos taurus*). J. Parasitol., **91**, 624–629.

Fayer, R., Trout, J.M., Xiao, L., Morgan, U.M., Lal, A.A., Dubey, J.P., 2001. *Cryptosporidium canis* n. sp. from domestic dogs. J. Parasitol. **87**, 1415–1422.

Fichtenbaum, C.J., Ritchie, D.J., Powderly, W.G., 1993. Use of paromomycin for treatment of cryptosporidiosis in patients with AIDS. Clin Infect Dis **16**, 298–300.

García-Estrada, C., C.F. Prada, C., Fernández-Rubio, F., Rojo-Vázquez, Balaña-Fouce, R., 2010. DNA topoisomerases in apicomplexan parasites: promising targets for drug discovery. Proc Biol Sci **277**, 1777-1787.

Gargala G. 2008. Drug treatment and novel drug target against *Cryptosporidium*. Parasite **5**, 275-81.

Gargala, G., Le Goff, L., Ballet, J.-J., et al., 2010. Evaluation of new thiazolide/thiadiazolide derivatives reveals nitro group-independent efficacy against *in vitro* development of *Cryptosporidium parvum*. Anitmicrob. Agents Chermother. **54**, 1315-1318.

Gatei, W., Wamae, C.N., Mbae, C., Waruru, A., Mulinge, E., Waithera, T., Gatika, S.M., Kamwati, S.K., Revathi, G., Hart, C.A., 2006. Cryptosporidiosis: prevalence, genotype analysis and symptoms associated with infections in children in Kenya. Am. J. Trop. Med. Hyg. **75**, 78–82.

Gilles, H.M., Hoffman, P.S., 2002. Treatment of intestinal parasitic infections: a review of nitazoxanide. Trends Parasitol. **18**, 95-97.

Girouard, D., Gallant, J., Akiyoshi, D.E., Nunnari, J., Tzipori, S., 2006. Failure to propagate Cryptosporidium spp. in cell-free culture. J. Parasitol. **92**, 399–400.

Gomez-Morales, M.A., 2004. [Highly Active AntiRetroviral Therapy and cryptosporidiosis]. Parassitologia **46**:95-99.

Gomez-Morales, M.A., Mele, R., Ludovisi,A., Bruschi, F., Tosini, F., Rigano, R., Pozio, E., 2004. Cryptosporidium parvum-specific CD4 Th1 cells from sensitized donors responding to both fractionated and recombinant antigenic proteins. Infect. Immun. **72**, 1306-1310.

Goodgame R. W., Understanding intestinal spore-forming protozoa: Cryptosporidia, microsporidia, isospora, and. Ann. Intern. Med., **124**, 429-441.

Griffiths, J.K., Moore, R., Dooley, S., Keusch, G.T., Tzipori, S., 1994. *Cryptosporidium parvum* infection of Caco-2 cell monolayers induces an apical monolayer defect, selectively increases transmonolayer permeability, and causes epithelial cell death. Infect. Immun. **62**, 4506–4514.

Guerrant, R.L., 1997. Cryptosporidiosis: an emerging, highly infectious threat. Emerg. Infect. Dis. **3**, 51.

Guselle N., 1999. Giardia Cyst and *Cryptosporidium* Oocyst Survival in Water, Soil, and Cattle Feces. J. Environ. Qual. **28**:1991-1996.

Hammond, T.G., Benes, E., O'Reilly, K.C., Wolf, D.A., Linnehan, R.M., Taher, A., Kaysen, J.H., Allen, P.L., Goodwin, T.J. 2000. Mechanical Culture Conditions Effect Gene Expression: Gravity-Induced Changes on the Space Shuttle. Physical Genomics **3**, 163-173.

Hampton, J. C., Rosario, B., 1966. Ultrastructural study of *Crytosporidium* development in Madin-Darby canine kidney cells J. Parasitol. **52**, 939-949.

Harris J. R., Petry F., 1999. *Cryptosporidium parvum*: structural components of the oocyst wall. J. Parasitol. **85**, 839-849.

Health Protection Agency, Health Protection Report, 2013. Outbreak of cryptosporidiosis in England and Scotland, May 2012. Retrieved from Health Protection Agency website:
http://www.hpa.org.uk/hpr/news/default_0413_aa_crptsprdm.htm

Hewitt, R.G., Yiannoutsos, C.T., Higgs, E.S., et al., 2000. Paromomycin: no more effective than placebo for treatment of cryptosporidiosis in patients with advanced human immunodeficiency virus infection. AIDS Clinical Trial Group. Clin. Infect. Dis. 31, 1084–1092.

Hijjawi, N.S. 2010. *Crypstosporidium*: New Developments in Cell Culture. Exp. Parasitol. **124**, 54-60.

Hijjawi, N.S., Meloni, B.P., Ryan, U.M., Olson, M.E., Thompson, R.C.A., 2002. Successful *in vitro* cultivation of *Cryptosporidium andersoni:* evidence for the

existence of novel extracellular stages in the life cycle and implications for the classification of *Cryptosporidium*. Int. J. Parasitol. **32**, 1719–1726.

Huang, D.B., White, A.C., 2006. An updated review on *Cryptosporidium* and *Giardia*. Gastroenterol. Clin. N. Am. **35**, 291–314.

Hunter, P.R., Hughes, S., Woodhouse, S., Raj, N., Syed, Q., Chalmers, R.M., Verlander, N.Q., Goodacre, J., 2004. Health sequelae of human cryptosporidiosis in immunocompetent patients. Clin. Infect. Dis. **39**, 504–510.

Hoxie, N.H., Davis, J.P., Vergeront, J.M., Nashold, R.D., & Glaier, K.A., 1997. Cryptospoiridiosis-associated mortality following a massive waterborne outbreak in Milaukee, Wisconsin. Am J Public Health. **87**, 2032–2035.

Hunter, P.R., Nichols, G., 2002. Epidemiology and clinical features of *cryptosporidium* infection in immunocompromised patients. Clin. Microbiol. Rev. **15**, 145-154.

Iseki, M., 1979. *Cryptosporidium felis* sp. n. (Protozoa: Eimeriorina) from the domestic cat. Jap. J. Parasitol. **28**, 285–307.

Itakura C., Nakamura H., Umemura T. & Goryo M., 1985. Ultrastructure of cryptosporidial life cycle in chicken host cells. Avian Path. **14**, 237-249.

James A. Ernest, Byron L. Blagburn, David S. Lindsay, William L., 1986. Infection dynamics of *Cryptosporidium parvum* (Apicomplexa: cryptosporiidae) in neonatal mice (*Mus musculus*). J. Parasitol. **72**, 796-798.

Jenkins, M.B., Eaglesham, B.S., Anthony, L.C., Kachlany, S.C., Bowman, D.D., Ghiorse WC., 2010. Significance of wall structure, macromolecular composition, and surface polymers to the survival and transport of *Cryptosporidium parvum* oocysts. Appl. Environ. Microbiol. **76**, 1926-34.

Jirků, M, Valigurová, A., Koudela, B., Krízek, J., Modrý, D., Slapeta J., 2008. New species of *Cryptosporidium* Tyzzer, 1907 (Apicomplexa) from amphibian host: morphology, biology and phylogeny. Folia Parasitol. **55**, 81-94.

Jokipii, L., Jokipii, A.M.M., 1986. Timing of symptoms and oocyst excretion in human cryptosporidiosis. New Eng. J. Med. **315**, 1643–1647.

Kopecna´, J. et al., 2006. Phylogenetic analysis of coccidian parasites from invertebrates: search for missing links. Protist **157**, 173–183.

Kosek, M., Alcantara, C., Lima, A. A., Guerrant, R. L., 2001. Cryptosporidiosis: an update. Lancet Infect. Dis. **1**,262-9.

Koudela, B., Modry, D., 1998. New species of *Cryptosporidium* (Apicomplexa, Cryptosporidiidae) from lizards. Folia Parasitologia **45**, 93–100.

Langer, R.C., Riggs, M.W., 1999. *Cryptosporidium parvum* apical complex
  glycoprotein CSL contains a sporozoite ligand for intestinal epithelial cells. Infect.
  Immun. **67**, 5282–5291.

**Leav, B.A., Yoshida, M., Rogers, K., Cohen, S., Godiwala, N., Blumberg, R S.,
  Ward, H.**, 2005. An early intestinal mucosal source of gamma interferon is
  associated with resistance to and control of *Cryptosporidium parvum* infection in
  mice. Infect Immun. **73**, 8425-8.

Levine N. D., 1980. Some Corrections of Coccidian (Apicomplexa: Protozoa)
  Nomenclature. J. Parasitol. **66**, 830-834.

Levine , N. D., The Protozoan Phylum Apicomplexa*, Vol. 2.* CRC Press*, Boca Raton,*
  1988.

**Lindsay, D.S., Upton, S.J., Owens, D.S., Morgan, U.M., Mead, J.R., Blagburn,
  B.L.,** 2000. *Cryptosporidium andersoni* n. sp. (Apicomplexa: Cryptosporiidae)
  from cattle, *Bos taurus*. J. Euk. Microbiol. **47**, 91–95.

**Liu, J., Deng, M., Lancto, C. A., Abrahamsen, M. S., Rutherford, M. S.,
  Enomoto, S**., 2009. Biphasic modulation of apoptotic pathways in
  Cryptosporidium parvum-infected human intestinal epithelial cells. Infect.
  Immun., **77**, 837-49.

Liu, J., Enomoto, S., Lancto, C.A., Abrahamsen, M.S., Rutherford, M.S., 2008. Inhibition of apoptosis in *Cryptosporidium parvum* infected intestinal epithelial cells is dependent on survivin. Infect. Immun. **76,** 3784–3792.

MacKenzie, W.R., Hoxie, N. J., Proctor, M. E., Gradus, M. S., Blair, K. A., Peterson, D. E., Kazmierczak, J. J., Addiss, D. G., Fox, K. R., Rose, J. B,. 1994. A massive outbreak in Milwaukee of *Cryptosporidium* infection transmitted through the public water supply. N. Engl. J. Med. **331**, 161-167.

MacKenzie, W.R., Schell, W. L., Blair, K. A., Addiss, D. G., Peterson, D. E., Hoxie, N. J., Kazmierczak, J. J., Davis, J. P., 1995. Massive outbreak of waterborne *Cryptosporidium* infection in Milwaukee, Wisconsin: recurrence of illness and risk of secondary transmission. Clin Infect Dis **21**, 57-62.

McDougald L. R., and Jeffers T. K., 1976. *Eimeria tenella* (Sporozoa, Coccidia): Gametogony following a single asexual generation. Science **192**: 258-259.

McLauchlin, J., Amar, C., Pedraza-Diaz, S., Nichols, G.L., 2000. Molecular epidemiological analysis of *Cryptsosporidium* spp. In the United Kingdom: results of genotyping *Cryptosporidium* spp. In 1705 fecal samples from humans and 105 fecal samples from livestock animals. J. Clin. Microbiol. **38**, 3984-3990.

Meisel, J.L., Perera, D.R., Meligro, C., Rubin, C.E., 1976. Overwhelming watery diarrhea associated with a *Cryptosporidium* in an immunosuppressed patient. Gastroenterol. **70**, 1156–1160.

Montalbano, M.A., Knowles, C.M., Adams, D.A., Hall, P.A., Fagan, R.F., Brendel, K.A., Holden, H.R., Jones, G.F., et al., 1997. Summary of Notifiable Diseases, United States 1996. MMWR **45**, 1-87.

Morgan-Ryan, U.M., Fall, A., Ward, L.A., Hijjawi, N., Sulaiman, I., Fayer, R., Thompson, R.C., Olson, M., Lal, A., Xiao, L., 2002. *Cryptosporidium hominis* n. sp. (Apicomplexa: Cryptosporidiidae) from *Homo sapiens*. J. Euk. Microbiol. **49**, 433–440.

Nelson, J.B., O'Hara, S.P., Small, A.J., Tietz, P.S., Choudhury, A.K., Pagano, R.E., Chen, X.M., Larusso, N.F., 2006. Cryptosporidium parvum infects human cholangiocytes via sphingolipid-enriched membrane microdomains. Cell Microbiol. **8**, 1932-1945.

Nime, F.A., Burkek, J.D., Page, d.L., Holscher, M.A., Yardley, J.H., 1976. Acute enterocolitis in a human being infested with the protozoan *Cryptosporidium*. Gastroenterol. **70**, 592-598.

O'Donoghue, P.J., 1995. *Cryptosporidium and* cryptosporidiosis in man and animals. Int. J. Parasitol. **25**, 139-195.

O'Hara S. P., B. Q. Huang, X. M. Chen, J. Nelson, N. F. LaRusso. 2005. Distribution of *Cryptosporidium parvum* sporozoite apical organelles during attachment to and internalization by cultured biliary epithelial cells. J Parasitol **91**:995-999.

Ostrovska K., Paperna I. 1990. *Cryptosporidium* sp. Of the starred lizard *Agama stellio*: ultrastructure and life cycle. Parasitol. Res. **76,** 712-720.

Pavlásek, I., 1999. Cryptosporidia: biology, diagnosis, host spectrum specificity and the environment. Klinicka Mikrobiologie a Infekcni Lekarstvi **3**, 290–301.

Pavlásek, I., Lávicková, M., Horák, P., Král, J., Král, B., 1995. *Cryptosporidium varanii* n.sp. (Apicomplexa: Cryptosporidiidae) in Emerald monitor (*Varanus prasinus* Schlegal, 1893) in captivity in Prague Zoo. Gazella **22**, 99–108.

Petersen, C., et al., 1992. Identification and initial characterization of five *Cryptosporidium parvum* sporozoite antigens genes. Infect. Immun. **60**, 2343–2348.

Plattner, F., Soldati-Farve, D., 2008. Hijacking of host cellular functions by the Apicomplexa. Ann. Rev. Microbiol. **62**, 471-487.

Pohlenz, W., Bemrick, J., Moon, H.W., and Cheville, N.F., 1978. Bovine Cryptosporidiosis: A Transmission and Scanning Electron Microscopic Study of Some Stages in the Life Cycle and of the Host-Parasite Relationship. Vet. Pathol. **15**, 417-427.

Power, M., Ryan, U., 2008. *Cryptosporidium macropodum* n. sp. (Apicomplexa: Cryptosporidiidae) from eastern grey kangaroos *Macropus giganteus*. J. Parasitol. **94**, 1114–1117.

Ramirez, N.E., Ward, L.A. and Sreevatan, S., 2004. A review of the biology and epidemiology of cryptosporidiosis in humans and animals. Microbes Infect. **6**, 773–785.

Reduker, D. W., Speer, C. A., Blixt, J. A., 1985. Ultrastructure of *Cryptosporidium parvum* oocysts and excysting sporozoites as revealed by high resolution scanning electron microscopy. J. Euk. Microbiol. **32**, 708-711.

Rider S. D., and G. Zhu., 2008. Differential expression of the two distinct replication protein A subunits from Cryptosporid*ium parvum*. J Cell Biochem **104,** 2207-2216.

Riggs, M.W. et al., 1999. *Cryptosporidium parvum* sporozoite pellicle antigen recognised by a neutralizing monoclonal antibody is a b-mannosylated glycolipid. Infect. Immun. **67**, 1317–1322.

Robertson, B., Sinclair, M.I., Forbes, A.B., Veitch, M., Kirk, M., Cunliffe, D., Willis, J., Fairley, C.K., 2002. Case-control studies of sporadic cryptosporidiosis in Melbourne and Adelaide, Australia. Epidemiol. Infect. **128**, 419–431.

Robson, K.J., Dolo, A., Hackford, I.R., Doumbo, O., Richards, M.B., Keita, M.M., Sidibe, T., Bosman, A., Modiano, D., Crisanti, A., 1998. Natural polymorphism in the thrompospondin-related adhesive protein of *Plasmodium falciparum*. Am. J. Trop. Med. Hyg. **58**, 81-89.

Rosales, M.J., Cordon, G.P., Moreno, M.S., Sanchez, C.M., 2005. Extracellular like-gregarine stages of *Cryptosporidium parvum.* Acta Tropica **95**, 74–78.

Rossignol J. F., 2010. *Cryptosporidium* and *Giardia:* treatment options and prospects for new drugs. Exp. Parasitol. **124**, 45-53.

Ryan, U., O'Hara, A., Xiao, L., 2004. Molecular and biological characterization of a *Cryptosporidium molnari*-like isolate from a guppy (*Poecilia reticulate*). Appl. Env. Microbiol. **70**, 3761–3765.

Ryan, U.M., Power, M., Xiao, L., 2008. *Cryptosporidium fayeri* n. sp. (Apicomplexa: Cryptosporidiidae) from the Red Kangaroo (*Macropus rufus*). J. Euk. Microbiol. **55**, 22–26.

Ryan, U.M., Xiao, L., Read, C., Sulaiman, I.M., Monis, P., Lal, A.A., Fayer, R., Pavlásek, I., 2003. A redescription of *Cryptosporidium galli* Pavlasek, 1999 (Apicomplexa: Cryptosporidiidae) from birds. J. Parasitol. **89**, 809–813.

Sibley, L.D., 2004. Intracellular parasite invasion strategies. Science **304**, 248–253.

Sickness bug found in tap water., 2008. BBC News. Retrieved from http://news.bbc.co.uk/2/hi/uk_news/england/northamptonshire/7472619.stm Retrieved from web 10/13/12.

Slavin, D., 1955. *Cryptosporidium meleagridis* (sp. nov.). J. Comp. Pathol. **65**, 262–266.

Smith, H. V., R. A. Nichols, A. M. Grimason., 2005. *Cryptosporidium* excystation and invasion: getting to the guts of the matter. Trends Parasitol. **21**, 133–142.

Spano, F., Putignani, L., McLauchlin, J., Casemore, D.P., Crisanti, A., 1997. PCR-RFLP analysis of the *Cryptosporidium* oocyst wall protein (COWP) gene discriminates between *C. wrairi* and *C.parvum*, and between *C. parvum* isolates of human and animal origin. FEMS Microbiol. Lett. **150**, 209–217.

Templeton, T.J., Kaslow, D.C., 1997. Cloning and cross-species comparison of the thrombospondin-related anonymous protein (*TRAP*) gene from *Plasmodium knowlesi, Plasmodium vivax,* and *Plasmodium gallinaceum*. Mol. Biochem. Parasitol. **84**, 13-24.

Templeton, T.J., Lancto, C.A., Vigdorovich, V., Liu, C., London, N.R., Hadsall K.Z., Abrahamsen, M.S., 2004. The *Cryptosporidium* oocyst wall protein is a member of a multigene family and has a homolog in *Toxoplasma*. Infect. Immun. **72**, 980-987.

Theodos CM, Griffiths JK, D'Onfro J, Fairfield A, Tzipori S, 1998. Efficacy of nitazoxanide against *Cryptosporidium parvum* in cell culture and in animal models. Antimicrob. Agents Chemother. **42**, 1959–1965.

Thompson R. C., Olson M. E., Zhu G., Enomoto S., Abrahamsen M. S., Hijjawi, N. S., 2005. *Cryptosporidium* and cryptosporidiosis. Adv. Parasitol. **59**, 77-158.

Tyzzer, E.E., 1907. A sporozoön found in the peptic glands of the common mouse. Proc.Soc. Exp. Bio. and Med. **5**, 12-13.

Tyzzer, E.E., 1910. An extracellular coccidium, *Cryptosporidium muris* (gen. et sp.nov.), of the gastric glands of the common mouse. J. Med. Res. **18**, 487-509.

Tyzzer, E.E., 1912, *Cryptosporidium parvum* (sp.nov.), a coccidium found in the small intestine of the common mouse. Arch. Protistenk. **26**, 394-412.

Tzipori, S., Griffiths, J.K., 1998. Natural history and biology of *Cryptosporidium parvum*. Adv. Parasitol. **40,** 5–36

Valigurová A., Jirků M., Koudela B., Gelnar M., Modrý D., Slapeta J., 2008. Cryptosporidia: epicellular parasites embraced by the host cell membrane. Int. J. Parasitol. **38,** 913-22.

Vetterling, J.M., Jervis, H.R., Merrill, T.G., Sprinz, H., 1971. *Cryptosporidium wrairi* sp.n. from the guinea pig *Cavia porcellus*, with an emendation of the genus. J. Protozool. **18**, 243–247.

Ward, W., Cevallos, A.M. 1998. *Cryptosporidium*: molecular basis of host–parasite interaction. Adv. Parasitol. **40**, 152–185.

Warren, C.A., Destura, R.V., Emmanuel, J., Sevileja, A.D., Barroso, L.F., Carvalho, H., Barret, L.J., O'Brein, A.D., Guerrant, R.L. 2008. Detection

of Epithelial-Cell Injury, and Quantification of Infection, in the HCT-8 Organoid Model of Cryptosporidiosis. J. Inect. Dis. **198**, 143-149.

Wilczynski, J., Ives, R., Peters, S., Henderson, T., Schneeberger, C., Xiao, L., Dearen, T., Webeck, J. Outbreak of Cryptosporidiosis Associated with a Firefighting Response — Indiana and Michigan, June 2011. MMWR, **61**, 153-156.

Xiao, L., Bern, C., Limor, J., *et al.***,** 2001. Identification of 5 types of *Cryptosporidium* parasites in children in Lima, Peru. J. Infect. Dis. **183**, 492-497.

Xiao,. L., Escalante, L., Yang, C., Sulaiman, I., Escalante, A.A., Montali, R.J., Fayer, R., Lal, A.A., 1999. Phylogenetic analysis of *Cryptosporidium* parasites based on the small-subunit rRNA gene locus. Appl. Environ. Microbiol. **65**, 1578-1583.

Xiao, L., Fayer, R., Ryan, U., Upton, S.J., 2004. *Cryptosporidium* taxonomy: recent advances and implications for public health. Clin. Micro. Rev. **17**, 72–97.

Yoder, J.S., Harral, Courtney, Beach, M.J., 2010. Cryptosporidiosis surveillance – United States, 2006-2008. MMWR, 53(SS-8), 1–21.

Yu, Q., Li, J., Zhang, X., Gong, P., Zhang, G., Li, S., Wang, H., 2010. Induction of immune responses in mice by a DNA vaccine encoding *Cryptosporidium parvum* Cp12 and Cp21 and its effect against homologous oocyst challenge. Vet. Parasitol. **172**, 1-7

Zu, S.X., Fang, G.D., Fayer, R., Guerrant, R.L., 1992. Cryptosporidiosis: Pathogenesis and immunology. Parasitol. Today **8**, 24-27.

Zhang, L., Sheoran, A.S., Widmer, G., 2009. *Cryptosporidium parvum* DNA replication in cell-free culture. J Parasitol **95**:1239-1242.

Zhou, L., Singh, A., Jiang, J., Xiao, L., 2003. Molecular surveillance of Cryptosporidium spp. in raw wastewater in Milwaukee: implications for understanding outbreak occurrence and transmission dynamics. Journal of clinical microbiology **41**, 5254-5257.

CHAPTER 1: UTILIZATION OF A FETAL MOUSE MODEL OF

CRYPTOSPORIDIOSIS FOR IMMUNE STUDIES

Introduction

Cryptosporidium parvum is a zoonotic species that primarily infects humans and young calves of domestic cows, causing the diarrheal disease cryptosporidiosis (O'Donoghue, 1995, Thompson et al., 2005). This organism is difficult to study in the laboratory setting due in large part to the lack of productive infection models with which the life cycles of the human pathogen can be studied under experimental conditions. Laboratory rodents older than 3 weeks do not develop *C. parvum* infections and do not shed oocysts (Ernest, 1986). Larger animals, such as rabbits, canines, or non-human primates, do not produce an active infection when exposed to *C. parvum*. While they are used to propagate infectious oocysts for commercial research purposes, calves are not cost-effective research laboratory subjects due to the size of the animals and the high price of housing and upkeep. Further, the large volume of diarrhea produced in an active infection, high concentration of oocysts in the calves' feces, and contamination of the animals' hides with infectious organisms presents a particular safety concern for transmission to animal care workers.

Laboratory mouse models of *C. parvum* infection require either the use of neonates less than 3 weeks old or knockout mice with compromised immunity (Ungar, 1990). Knockout mice are not an ideal choice, due to the fact that the immune response is impacted by the lack of important components, thus presenting a skewed view of the disease process within a host. A neonatal mouse model can be a useful tool for observing pathological changes within the intestine and other immune responses. However, these animals are difficult to work with due to their small size and the delicacy required handling them without harming them.

To evaluate a murine laboratory model for future work elucidating the immunological reaction of the host to the parasite, we initiated a short-term neonatal mouse model using 21-day-old BALB/c mice. Two days after inoculation with *C. parvum* oocysts, the mice were euthanized. The distal ileum of each animal was cut into 0.5-cm segments, mounted in paraffin, and cut into 5-μm sections. Changes in the infected mouse intestine were then observed by light microscopy using various staining techniques.

Materials and methods

Animals and institutional use compliance

BALB/c mice were obtained from Jackson Laboratories (Bar Harbor, ME). Animals were housed in a specific pathogen-free facility with ad libitum access to food and water on a 12-h light:dark cycle. All experiments were performed in accordance with guidelines set forth by the Institutional Animal Care and Use Committee (IACUC) of North Dakota State University.

Infection of neonatal mice with C. parvum

One mouse was administered 0.2 mL sterile PBS via gastric gavage with a blunt 18-gauge needle to serve as an uninfected control. Each of the other two mice was administered 1×10^7 *C. parvum* oocysts in 0.2 mL sterile PBS in the same manner to establish experimental infection animals.

Collection and preparation of tissue samples from neonatal mice

At 24 h post-infection, all three mice were euthanized and the small intestine was dissected from each mouse. The terminal 60% of the ileum was flushed with sterile PBS, using a sterile syringe and blunted needle. This was followed by a 10% formalin flush. The intestine sections were fixed in 10% formalin solution for approximately 5 h. Specimens

53

were cut into 0.5-cm sections, and several sections were embedded on end in a single paraffin block, which was then cut into cross-sectional 5-μm slices and mounted on glass microscope slides for evaluation. Paraffin embedding and sample preparation was done by the NDSU VDL histology lab. Deparaffinized and dehydrated tissue slides were obtained for tissues from each mouse. Representative sections from each mouse were stained with hematoxylin and eosin (H&E). Slides were stored at 4°C until they were viewed under transmitted light microscopy for evidence of infection.

Lectin-VVL staining of tissue sections

In the initial staining procedures, a Lectin VVL-biotin (Vector Laboratories, Burlingame, CA) kit that was successfully used to stain *Cryptosporidium* intracellular stages in cell-culture monolayers was used to stain the murine intestine sections. However, the non-specific staining of mouse epithelial tissues resulted in an unacceptable level of background staining. The procedure was modified to include avidin/biotin-blocking steps, using reagents provided in the AEC-HRP Cell and Tissue Staining kit (R&D Systems, Minneapolis, MN) in an attempt to reduce background. While gains were made in reducing background staining, a protocol for staining the tissue sections with lectin for *C. parvum* without significant background staining was not perfected, and further optimization would be necessary to use this in tissue samples. The results are included to show the attempted optimization of the staining protocols.

Tissue sections affixed to glass slides were circled with a hydrophobic PAP pen (Abcam, Cambridge, MA) to provide a barrier for reagents. Several drops of 1% Triton X-100® (Union Carbide, Greensburg, LA) in PBS were added to cover the tissue sections. Slides were incubated at room temperature for 10 min. The Triton X-100® solution was removed before blocking.

Tissues were blocked with a bovine serum albumin (BSA) solution to prevent non-specific binding. Several drops of 0.5% BSA in PBS were added to cover each section, and the slides were incubated for 10 min at room temperature. The blocker was removed and four rinses of 3-4 drops of PBS was added to each section then removed by vacuum pipet.

Non-specific binding of lectin was blocked using the avidin-blocking reagent from the Cell and Tissue Staining kit (R&D Systems). This step was used to bind any endogenous avidin-binding sites in the tissue. Three to four drops of avidin blocking reagent were added to each section and incubated for 15 min at room temperature. This was followed with three rinses with the buffer supplied in the Cell and Tissue Staining kit (R&D Systems).

Following avidin blocking, the tissues were incubated with biotin to saturate any free biotin-binding sites on the avidin. Three to four drops of biotin blocking reagent were added to each tissue section and incubated at room temperature for 15 min. The blocking reagent was removed, and tissues were rinsed three times with rinse buffer.

Lectin-VVL, isolated from *Vicia villosa* (hairy vetch) seeds binds to certain surface glycoproteins on *Cryptosporidium parvum*. Using biotinylated lectin-VVL (R&D Systems), it is possible to stain cell cultures to observe infected cells and *Cryptosporidium* morphology. Lectin-VVL-biotin was added to each tissue section and incubated at room temperature for 30 min. The solution was removed and the slides were rinsed three times with PBS.

To avoid quenching the fluorescent label, the overhead lights were turned off in the lab for the following step, and the procedure was carried out in the ambient light from a window in the lab. Streptavidin-CY3 reagent (R&D Systems) was added to the tissue sections and incubated in the dark at room temperature, for 30 min. The reagent was removed and slides were rinsed once with PBS. Slides were protected from light and stored at 4°C when not being viewed.

Immunohistochemical staining of tissue sections

Immunohistochemical staining was carried out using a mouse anti-*C. parvum* Ab received from A. Sheoran, Tufts University in North Grafton, Massachusetts. Slides were placed in slide holders and loaded into a microwave pressure cooker. The pressure cooker was filled with 1.5 L 10-mM citric acid and locked. The pressure cooker was microwaved until one minute after the pressure indicator stem popped. The pressure cooker was removed from the microwave and allowed to sit for 10 min. The top was then removed, and the pressure cooker was allowed to cool for another 20 min.

After cooling, the slides were removed, and the samples were covered with 100 μL peroxidase blocker (R&D Systems) for 30 min at room temperature, after which slides were rinsed for 5 min in rinse buffer (PBS + 0.05% Tween20, VWR, Aurora, CO) on a rocker for agitation. The slides were then incubated with a serum-blocking reagent (R&D Systems). Reagent was removed, and the sample was quickly washed in rinse buffer. Avidin blocking reagent (R&D Systems) was added, and the samples were incubated at room temperature for 15 min, and then rinsed in PBS. The final blocking reagent, biotin-blocking reagent (R&D Systems) was added to the sample for 15 min at room temperature. This was rinsed off and excess buffer was blotted.

The samples were covered with mouse anti-*C. parvum* polyclonal Abs which had been diluted 1:5 in Ab diluent (Appendix) then incubated overnight at room temperature. Three 15-min washes in rinse buffer were used to remove excess primary Ab. The secondary Ab was biotinylated goat anti-mouse IgG diluted 1:200 in Ab diluent (R&D Systems). The slides were incubated at room temperature for 30 min and then washed 3 times for 15 min each in rinse buffer.

High sensitivity streptavidin (HSS) conjugated to horseradish peroxidase (HRP, R&D Systems) was added to the tissue sections and allowed to incubate at room temperature for 30 min. This was followed by three, 2-min washes in rinse buffer. HSS

has high affinity and specificity for the biotinylated secondary Ab, while the HRP causes an enzymatic reaction with the chromogen, allowing visualization of the labeled cells. The 3-amino,9-ethyl-carbazole (AEC) chromogen was mixed with the chromogen buffer (R&D systems) immediately before use. Several drops of the chromogen solution were added to cover the tissue specimens. The HRP-catalyzed reaction of AEC produced a dark pink pigment. Development was monitored under a microscope until the pigment was dark enough to be easily observed. The slides were rinsed in distilled water, followed by a 5-min distilled water wash. A 10-sec dip in Gill's hematoxylin III (Surgipath, Richmond, VA) was used to counterstain the sections. This was followed with two, 2.5-min washes in water. Cover slips were mounted with Aqueous Mounting Medium (Vector Labs) and dried vertically on a paper towel.

Results

H&E staining

     Cryptosporidium infection may cause intestinal villi blunting in infected mice (Garza, et al 2008). H&E-stained sections were evaluated for physical changes, and the gross anatomy of naïve and infected intestines were compared. Intestines from naïve mice showed long, narrow villi with sharp distal points (Fig 7A), while the villi from the infected mice appeared shorter and blunter (Fig 7B), even in sections where no *Cryptosporidium* cells were observed. The intestines from the infected mice also had irregular margins that were distorted, compared to the naïve mouse (Fig 7). Figure 8 shows *C. parvum* oocysts visible in intestinal crypts on the H&E-stained sections of intestine from the infected mouse at 100X and 200X magnification.
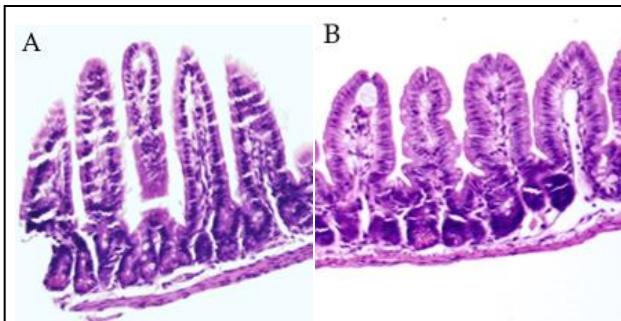
Figure 7. H&E-stained distal ilium from naïve neonatal or *C. parvum*-infected BALB/c mouse. The normal villi are regularly formed and narrow (A), while villi from mice inoculated with 1×10^7 *C. parvum* oocysts, 24 h post-infection are shorter with blunted ends. (B) Magnification 200X.
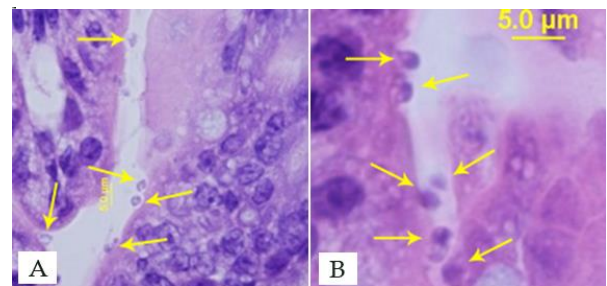
Figure 8. H&E-stained distal ilium from neonatal BALB/c mouse 24 h after being inoculated with 1×10^7 *C. parvum* oocysts. The yellow arrows indicate *C. parvum* oocysts in the intestinal crypts at 100X magnification (A) and at 200X magnification (B).
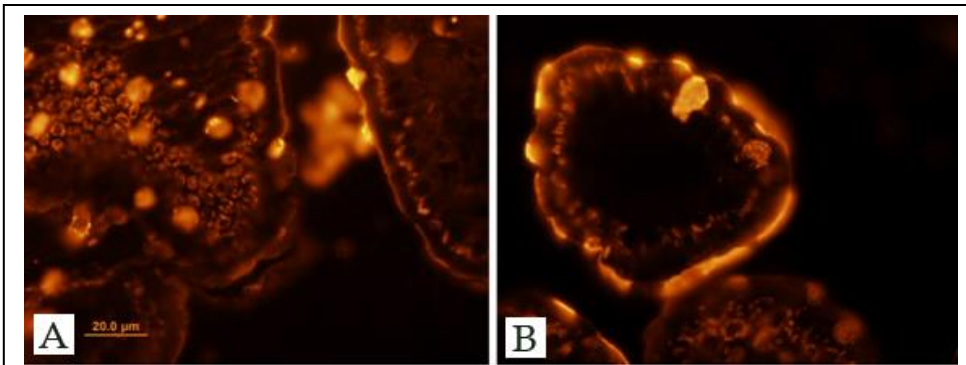
Figure 9. Lectin-VVL stain and modified Lectin-VVL stain of *C. parvum*-infected mouse intestines. The Lectin-VVL bound to the parasite and also to glycoproteins on the intestinal cells, causing background staining (A). Additional blocking did not decrease the background staining (B). Magnification 60X

Lectin-VVL staining

When stained using Lectin-VVL, the tissue sections showed unacceptable levels of non-specific staining (Fig 9A). Mouse tissue was labeled in many places, making identification of *C. parvum* difficult or impossible, due to the inability to differentiate between mouse tissues and *C. parvum*. Adding additional blocking steps did not result in an appreciable reduction in background, non-specific staining (Fig 9B).
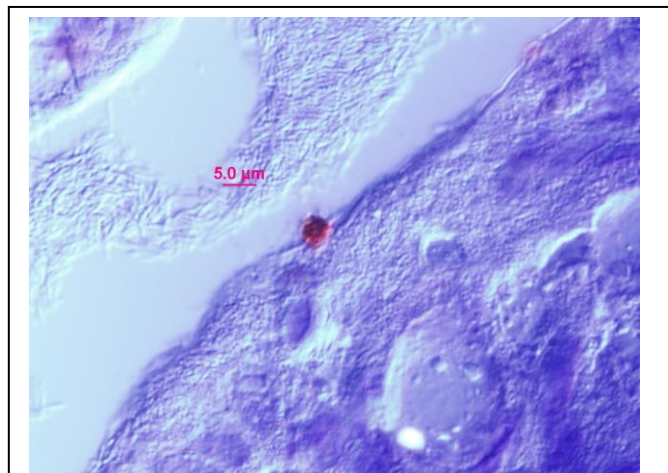
Figure 10. **IHC-stained tissue from *C. parvum*-infected BALB/c mouse ilium.** *C. parvum* was clearly visualized (pink, center of image), while mouse tissue remained unlabeled. Magnification 200X.

Immunohistochemical staining

The use of anti-*C. parvum* Ab in the IHC protocol yielded clear labeling of *C. parvum* within the tissue sections without background staining (Fig 10). This staining confirmed that the infected mouse intestines retained *C. parvum* two days following inoculation.

Discussion

Infection of neonatal mice and staining of tissues

In this study, we tested a neonatal model in anticipation of future studies that may be planned to characterize the host immune response to *C. parvum* infection. Oocyst shedding usually doesn't begin until at least the third day after infection; so the collection of fecal samples was not appropriate for this study (Petry, et al., 1995). However, we were able to document signs of infection in our mice at 24 h post-infection. We interpret the villi blunting (Fig 7) to suggest that this model would likely have become an active infection in the neonatal mouse.

The various staining methods tested on the tissue samples demonstrated the complexity of finding a marker that can identify *C. parvum* with minimal background binding to host cells. The first method used a lectin stain to bind glycoproteins. The basis of the lectin-VVL labeling for this stain is the presence of terminal N-acetyl-D-galactosamine residues (GalNAc). Unfortunately, GalNAc is also a component of intestinal goblet cells (Roth, 1984) and the lectin-VVL stain, which is effective in cell culture samples, had unacceptably high levels of non-specific binding. For the purpose of staining intestinal tissue sections after infection with *C. parvum* for immunological analysis or other studies, lectin-VVL staining is not a viable option.

Anti-*Cryptosporidium* IHC staining may be a more appropriate means for specific labeling of slide-mounted tissues. The Abs specific for *C. parvum* antigens used, with the staining parameters used did not demonstrate non-specific binding to host cells. We anticipate that as monoclonal Abs are developed for the various life stages of *C. parvum*, it will be possible to stain multiple life stages on the same sample, allowing researchers to more closely track the stages of infection.

With the advent of microdissection tools, such as Laser Capture Microdissection (LCM), identifying specific life stages will be necessary to ensure homogenous samples for analysis. As LCM techniques are perfected for dissecting single cells of interest, stage-specific genetic characterization may be possible. Methods for amplification of nucleic acids from single cells are currently being developed (Kurimoto, et al., 2006). This opens the door for future research exploring the molecular and cellular interaction between the parasite and its host. Identifying genetic markers for various stages of infection could lead to new directions in treatment of cryptosporidiosis.

Future directions

This model may be applicable for short-term immunological study. The infection method, although delicate, seems to be effective. There is the potential to develop an alternate method of infection, using a non-invasive protocol with droppers or nipples to allow the neonatal mice to ingest the oocysts. Infections allowed to progress for several days, up to several weeks, can allow the study of the changes in the intestines of the mice. Depending on the length of infection and development of the mouse, the immune system may be able to clear the infection itself. In that case, there would be opportunity to observe the immune response as it develops. Serological testing could include testing for regulation of various immune molecules.

Testing on tissue sections could be expanded to include IHC staining for specific inflammatory cells that may be migrating to the area, such as T cells. Testing for the presence of increased IgA on the mucosa could also indicate immune response in the host, although *in situ* testing for specificity may be a challenge. *Cryptosporidium* specific IgA, IgG and and IgM have been observed in experimental and naturally occurring infecitons of calves (Kassa, et al., 1991), so serum samples from the infected mice could be evaluated for immune response, as well.

Microdissection techniques can be employed to assess responses to *C. parvum* in infected cells, while using neighboring cells as controls. The regulation of host-cell apoptosis and other cell functions by *C. parvum* can also be monitored based on life stage differentiation and dissection of specific cells, either infected or non-infected. By being able to select cells that share a common infection status, gene regulation can be compared for cells within the same host. Using adjacent, uninfected cells in the same tissue sample as controls would be a marked advantage over using an uninfected host control.

Acknowledgements

References

Ernest, J.A., Blagburn, B.L., Lindsay, D.S., Current, W.L., 1986. Infection Dynamics of *Cryptosporidium parvum* (Apicomplexa: Cryptosporidiiae) in Neonatal Mice (*Mus musculus*). J. Parasitol. **72**, 796-798.

Garza A, Castellanos-Gonzalez A, Griffiths J, Robinson P., 2008. Infection of immunocompetent mice with acid-water-pretreated *Cryptosporidium parvum* results in weight loss, and intestinal (structural and physiological) alterations. Parasitol. Res. **102,**. 457-463.

Kassa, M, E Comby, D Lemeteil, P Brasseur, and J J Ballet., 1991. Characterization of anti-cryptosporidium iga antibodies in sera from immunocompetent individuals and hiv-infected patients. J Protozool **38** (6): 179S-180S

Kurimoto, K., Yabuta, Y., Ohinata, Y., Ono, Y., Uno, K., Yamada, R.G., Ueda, H.R., Saitou, M., 2006. An Improved Single-Cell cDNA Amplification Method for Efficient High-Density Oligonucleotide Microarray Analysis. Nucl. Acid. Red. **34**, e42.

O'Donoghue, P.J., 1995. *Cryptosporidium and* cryptosporidiosis in man and animals. Int. J. Parasitol. **25**, 139-195.

Petry F, Robinson HA, McDonald V., 1995. Murine infection model for maintenance and amplification of Cryptosporidium parvum oocysts. J Clin Microbiol. **95**, 1243-1246.

Roth, J., **1984.** Cytochemical localization of terminal N-acetyl-D-galactosamine residues in cellular compartments of intestinal goblet cells: implications for the topology of O-glycosylation. J. Cell. Biol. **98**, 399-406.

Thompson R. C., Olson M. E., Zhu G., Enomoto S., Abrahamsen M. S., Hijjawi, N. S., 2005. *Cryptosporidium* and cryptosporidiosis. Adv. Parasitol. **59**, 77-158.

Ungar, B.L., Burris, J.A., QUinn, C.A., Finkelman, F.D., 1990. New Mouse Models for Chronic *Cryptosporidium* Infection in Immunodeficient Hosts. Infect. Immun. **58**, 961-999.

CHAPTER 2: DEVELOPMENT OF A CELL-CULTURE METHOD ON FRAMESLIDES® FOR THE USE OF LASER MICRODISSECTION IN THE STUDY OF *CRYPTOSPORIDIUM* LIFE STAGES

Introduction

Cryptosporidium parvum is a zoonotic parasite that causes cryptosporidiosis. The hallmark of this disease is stomach discomfort and severe diarrhea lasting up to two weeks. The disease became prominent in the medical community when the increasing numbers of immunosuppressed persons, especially HIV/AIDS patients, began to develop chronic infections, sometimes causing death (Casemore, 1985, Guerrant, 1997). Laboratory study has proven difficult due to the lack of a satisfactory animal model of the disease.

Infection of cell cultures has allowed scientists to study the parasite's life stages, but with significant limitations. Some scientists have reported successful cultivation of *Cryptosporidium* in host cell-free culture, but this technique has not been replicated in other labs (Zhang, et al., 2009). The complex life cycle of *C. parvum* does not progress indefinitely in cell culture, and although all of the life stages of *C. parvum* have been observed in cell culture, serial passage has not been demonstrated.

Developing a method for positive identification of life cycles of *Cryptosporidium* will allow closer study of individual stages and ultimately can provide insight into the trigger for switching from asexual to sexual reproduction. This is an important trigger to understand, as it marks the point where the parasite begins to be shed in the feces of the host and potentially to be spread to secondary hosts. As such, the trigger for the switch to sexual reproduction may offer a target for chemotherapeutic agents against cryptosporidiosis. While cell culture does produce the various life stages of the parasite, including production of oocysts, there is no current method to accurately identify various

intracellular stages. Microscopic identification of Type I and Type II meronts is a subjective and time-consuming process. However, the potential for developing monoclonal antibodies for specific life-stages does exist if Type I and Type II meronts could be isolated and unique markers were found and exploited.

There are several cell lines that have been used to study *C. parvum*. Human ileocecal adenocarcinoma (HCT-8), stomach adenocarcinoma (AGS), and colorectal adenocarcinoma (Caco-2) are three lines of human cells that support growth of various *Cryptosporidium* species. The Madin-Darby canine kidney (MDCK) cell line is also commonly used for cell culture of *Cryptosporidium* (Yu, et al., 2000, Arrowood, 2002). MDCK cells are fast-growing, are not as fastidious as other cell lines, and provide a level cell monolayer in which to observe the *C. parvum* life cycle in a relatively constant focal plane, making them well-suited for this experiment. The NDSU DNA Forensic Laboratory provided use of the laser microdissection microscope for these experiments. As they were in the process of being accredited as a crime lab, an additional factor in choosing the non-human MDCK cells was that they would be an unlikely source of contamination for human forensics.

The guiding principles for this work were that cell culture in Chamber slides™ (Thomas Scientific, Swedesboro, NJ) would allow the side-by-side comparison of multiple variations of different factors, such as host cell density, infectious dose, and growth medium components. Following incubation, staining or immunohistochemistry (IHC) could be carried out on the chamber slides to allow observation and analysis. Host cells and *Cryptosporidium* cells could then be collected from individual chambers for analysis of gene expression under different conditions. However, one limitation of using a whole chamber for analysis is that it does not allow sorting of oocysts, meronts, merozoites, and host cells so it is not always certain which life stage is expressing the genes detected. For example, the control of host cell apoptosis is a function that is of particular interest to

researchers that is not well understood at present. It is known that *Cryptosporidium* can regulate host cell apoptosis, and targeted genetic analysis would provide insight into the genes that control this function (Liu, et al., 2008, Liu, et al., 2009, Plattner and Soldati-Favre, 2008).

Laser Capture Microdissection® (LCM) is a technology that can be used to discriminate between closely associated cells—for example, parasite-infected cells and their normal near neighbors or between different stages of parasite development *in situ*. Importantly, the ability to select a single, infected cell with LCM would enable genetic analysis of both host cells and *Cryptosporidium* cells in specific stages of infection. With LCM, individual cells may be collected based on specific parameters. The Positioning Ablation Laser MicroBeam® (PALM®) Micro-Laser system (P.A.L.M. Microlaser Technologies AG, Bernried, Germany) can be used to mark selected areas of a slide for collection. The selected cells can then be catapulted into the collection tube with focused laser energy. Once a sample is collected, DNA or RNA can be extracted from the cells for further experimentation. Capturing high quality nucleic acid is critically important to the quality of the data that can be generated from these experiments. Membrane-coated glass slides allow the laser to catapult cells from the slide without destroying the cell and with less damage to the cell's nucleic acid. In a similar way, FrameSlides® (Zeiss, Germany) have a membrane mounted on an open metal frame which allows the laser to cut around the selected cells and then to catapult them into the collection tube without damaging the cell or the genetic material within.

In order to use LCM with cell culture, cells must first be grown on the slides. Since flat microscope slides don't lend themselves to cell culture, a new method was needed. FrameSlides® are a unique construction in which a metal platform supports a membrane, forming a large shallow well. We exploited this design to repurpose the FlameSlide® for use in cell culture and subsequent infection with *Cryptosporidium*.

MDCK cells were cultured in both NUNC Lab-Tek I Chamber slides (Thomas Scientific, Swedesboro, NJ) and FrameSlides® (Zeiss, Germany) and infected with *C. parvum* oocysts. Lectin-VVL staining and immunohistochemical staining were performed on each type of slide. Microscopy was carried out on both an Olympus BX61 with a 12 mexapixel camera for capturing images and the Zeiss PALM system, which was equipped for fluorescent microscopy and image capture. Microscopic visualization of the fluorophor was successful only when used with cover slips and SlowFade® mounting medium (Molecular Probes, Eugene, OR). To allow laser microdissection, the SlowFade® and coverslip had to be left off and the fluorescent signal was quickly quenched when exposed on the PALM microscope without use of these protecting barriers. IHC-stained cells were easily observed under both microscopes and life stages were observed and recognized. Chamber slides were also stained with Sporo-Glo® (Waterborne Inc., New Orleans, LA) for observation under fluorescent microscopy.

Cryptosporidium life stages were photographed on Chamber Slides® using a 12 mega-pixel camera-equipped Olympus BX61 and oocysts were collected using LCM®. Samples containing up to 100 *C. parvum*-infected cells were collected with the PALM® system and RNA was extracted.

Materials and methods

In vitro *cultivation of Madin-Darby canine kidney cells on Chamber Slides®*

 Cells used for this experiment were obtained from ATCC and maintained in Dr. McEvoy's lab. All pertinent NDSU IBC protocols are followed in the use of these cell lines.

A monolayer of MDCK cells (ATCC CCL-34) was grown to confluence at 37ºC and 5% CO_2 and was used for subculture. Growth medium was removed and cells were rinsed with serum-free Minimal Essential Medium (MEM, Appendix). Six milliliters of 0.25%

trypsin (Gibco, Grand Island, NY) was added to the monolayer and incubated at room temperature for 15 min to detach cells from the flask. Once the monolayer was detached from the surface of the flask, the flask was knocked firmly on one side to dislodge the cells. Six milliliters of MEM with 10% FBS was added to the culture flask to suspend the cells and to inactivate the trypsin. A 100-μL aliquot of the cell suspension was added to 100 μL of trypan blue working solution (Appendix), and cells were counted using a hemacytometer. The cells were pelleted by centrifugation and resuspended at a concentration of 1.7×10^5 cells/mL in MEM plus 10% FBS.

NUNC Lab-Tek I Chamber slides (Thomas Scientific, Swedesboro, NJ) were seeded with 1 mL of the cell suspension and incubated for 24-48 h at 37°C and 5% CO_2 in a hydrated chamber. Cells were observed periodically using an inverted microscope to determine confluency. When an estimated 70%-80% of the chamber slide surface area was covered with MDCK cells, the cells were infected with oocysts.

Infection of MDCK cells in Chamber Slides® with C. parvum

C. parvum (Iowa isolate) oocysts were obtained from Waterbourne, Inc. (New Orleans, LA). The oocyst concentration was 6.25×10^5/mL in PBS with 1 mM Sigma A5955 antibiotic/antimycotic. For each sample, 8.0 μL of the oocyst suspension was added to a 1.5-mL centrifuge tube (5×10^4 oocysts/tube). The tubes were centrifuged at 20,000 $\times g$ for 3 min. The oocysts were then suspended in 200 μL of 10% (vol:vol) bleach solution and incubated for 10 min at 4°C. Following this incubation, cells were centrifuged at 20,000 $\times g$ for 3 min, and the supernatant was removed. Oocysts were washed in sterile PBS three times to remove the bleach. Following the third wash, oocysts were resuspended in 500 μL of infection medium (Appendix).

Chamber slides with monolayers of 70-80% confluent MDCK (ATCC CCL-34) cells were removed from the incubator and medium was removed. The infection medium

69

containing the oocysts was added to each well. A negative control well containing only infection medium and MDCK cells was included. Chamber slides were returned to the CO_2 incubator for 3 h to allow excystation and for the released sporozoites to infect the MDCK cells. Infection medium was removed and 1 mL MEM with 10% FBS was added to each well for incubation.

Cells were incubated for 24-48 h, the growth medium was removed, and cells were rinsed twice with 1 mL PBS. Cells were fixed for staining by incubating in 1 mL of 4% formaldehyde for 30 min at room temperature. This solution was removed and cells were washed twice in PBS.

Infection of MDCK cells with C. parvum *with bile-salt excystation*

An alternate excystation/infection protocol, based on current published literature showing an improved efficiency of excystation and infection by saving one step of handling, was trialed for this study. Briefly, the oocysts were incubated for 30 min at 37°C resuspended in a 0.8% solution of the bile salt sodium taurocholate (NaTC) following the bleach treatment and rinses. Following this incubation, cells were centrifuged at 20,000 $\times g$ for 3 min, and the supernatant was removed. Oocysts were washed in sterile PBS three times. Following the third wash, oocysts were resuspended in 500 μL of infection medium. Oocysts were resuspended in 1 mL of infection medium and the incubation was allowed to proceed uninterrupted. Subsequent steps of the protocol remained the same as the bleach treatment protocol. There was no observable difference in the results obtained from the two different infection protocols.

In vitro *cultivation of MDCK cells on FrameSlides®*

FrameSlides® (Zeiss, Germany) were used to enable the collection of *C. parvum* cells with the PALM® laser microdissection pressure catapulting microscope (Zeiss). Prior to cell culture, the FrameSlides were placed in a slide-holder and sterilized by

gamma irradiation in a [137]CsCl irradiator (dose 8600 Gy). The sterile FrameSlide® was removed from the container with sterile forceps and placed in a sterile Petri dish until use. A suspension of 1.7×10^5 MDCK cells/mL was prepared in MEM with 10% FBS. The FrameSlide® was carefully loaded with 1.4 mL of the cell suspension, allowing the growth medium to completely cover the membrane and well up above the side of the frame. The Petri dish containing the FrameSlide® was carefully placed in the 37°C incubator with 5% CO_2 and incubated overnight. The culture was observed periodically until the cells were 80% confluent on the membrane, and the FrameSlide® was prepped for infection as previously described for chamber slides. Extra care was needed when handling the slide to avoid spilling the medium. A PAP pen (Abcam, Cambridge, MA) was used to create a hydrophobic barrier around the edge of the FrameSlide® and minimize the spilling of culture medium. The PAP pen line was drawn slightly back from the edge of the membrane, to avoid possible chemical interaction with the membrane.

Infection of MDCK Cells on FrameSlides® with C. parvum

Oocysts were prepared using the bleach-only excystation technique above, and a 1.0 mL suspension of infection medium containing 1×10^6 oocysts was made. The growth medium was removed from the membrane slide and the oocyst suspension was added to the membrane. The culture was incubated at 37°C with 5% CO_2 for 48 h. It was necessary to change the infection medium after 24 h due to change in pH of the small volume of medium. When it started to turn orange/yellow, it was removed and replaced with MEM plus 10% FBS. At 48 h, the FrameSlides® were removed from the incubator, and the growth medium was removed. The cells were fixed with HistoChoice® (AMRESCO, Solon, OH) fixative for 30 min at room temperature, and the samples were stored at 4°C until use.

Lectin-VVL staining of infected MDCK cells

Monolayers on the FrameSlides® were permeabilized with 1 mL 1% TritonX-100®
(Union Carbide, Greensburg, LA) in PBS for 10 min at room temperature. One milliliter of
the TritonX-100® solution was added to each well and incubated at room temperature for
10 min. After permeabilization, the TritonX-100® solution was removed and the MDCK
cells were blocked with a solution of 0.5% bovine serum albumin (BSA) in PBS for 10 min
at room temperature to prevent non-specific binding.

Lectin VVL-biotin (Vector Laboratories) was diluted to a 1% w/v solution in PBS
containing 0.5% BSA and stored at -20°C until use. The working solution was thawed
before use, and 1 mL was added to each FrameSlide®and incubated for 30 min at room
temperature. After incubation, the lectin solution was removed and the FrameSlides®
were rinsed 3 times with 1 mL PBS.

Biotin-conjugated Lectin-VVL was labeled with conjugated Strepavidin-CY3
fluorophore, diluted to 1 μg/mL in PBS, by incubating at room temperature for 30 min
under low light to preserve this light-sensitive reagent. After incubation, cells were
washed twice with 1 mL PBS per chamber.

The chamber walls were removed from the slide, using the tool provided by the
supplier. To mount the cover slip, 8 μL Slow Fade mounting medium was added to each
chamber. The slides were stored at 4°C until used for microscopic analysis.

Sporo-Glo® staining of infected MDCK cells

Chamber slides were used to culture MDCK cells according to previous methods,
which were then infected with oocysts. Following removal of growth medium and rinsing
in PBS, slides were stained with Spro-Glo® (Waterborne, Inc., New Orleans, LA)
according to manufacturer's instructions. To mount the cover slip following staining, 8 μL
SlowFade® mounting medium was added to each chamber. Slides were stored at 4°C

until they were analyzed using fluorescence microscopy. The FITC filter was used to observe the cells.

Immunohistochemical staining of C. parvum-*infected MDCK cells on chamber slides*

MDCK monolayers growing on chamber slides were infected as described previously. Following incubation, growth medium was removed and cells were rinsed with MEM. Monolayers were fixed with HistoChoice® (Amresco, Solon, OH) for 30 min at room temperature. HistoChoice® was removed, and the plastic chambers were removed from the slides with the tool provided by the manufacturer.

The slides were incubated with a serum blocking reagent (R&D Systems). This reagent was removed, and the sample was quickly washed in rinse buffer. Avidin blocking reagent (R&D Systems) was added, and the samples were incubated at room temperature for 15 min, then rinsed in PBS. Biotin blocking reagent (R&D Systems) was added to the sample for 15 min at room temperature. The sample was rinsed, and excess buffer was removed by blotting.

The samples were incubated with mouse anti-*C. parvum* polyclonal Abs diluted 1:5 in Ab diluent (Appendix) overnight at room temperature. Three, 15-min washes in rinse buffer were used to remove excess primary Ab. The secondary Ab was biotinylated goat anti-mouse IgG diluted 1:200 in Ab diluents (R&D Systems). The slides were incubated at room temperature for 30 min and then washed 3 times for 15 min each in rinse buffer.

High sensitivity streptavidin (HSS), conjugated to horseradish peroxidase (HRP, R&D Systems) was added to the tissue sections and allowed to incubate at room temperature for 30 min. This was followed by three, 2-min washes in rinse buffer.

HSS has high affinity and specificity for the biotinylated secondary Ab, while the HRP causes an enzymatic reaction with the chromogen, allowing visualization of the labeled cells. The 3-amino,9-ethyl-carbazole (AEC) chromogen was mixed with the

chromogen buffer (R&D systems) immediately before use. Several drops of the chromogen solution were added to the tissue specimens. The HRP-catalyzed reaction of AEC produced a dark pink pigment. Development was monitored using bright field microscopy until the desired color intensity was achieved. The slides were rinsed in distilled water, followed by a 5-min distilled water wash. A 10-sec dip in Gill III hematoxylin (Surgipath, Richmond, VA) was used to counterstain the sections. This was followed with two, 2.5-min washes in water. Slides were cover-slipped using Aqueous Mounting Medium (Vector Labs) and dried vertically on a paper towel.

Staining C. parvum-*infected MDCK cells on FrameSlides®*

The lectin-VVL protocol that was used to stain chamber slide specimens was also used to stain fixed monolayers of MDCK cells. The only modifications to the protocol were that the volumes of the various liquid reagents were increased to 1.4 mL from 1.0 mL to account for the larger surface area and, following the final rinse, the FrameSlide® samples were not coverslipped, but were taken immediately to the LCM facility for laser dissection.

Immunohistochemical staining was also used on FrameSlide® samples. Again, reagent volumes were increased to account for increased sample surface area. Aliquots of 240 μL of each reagent were used to cover the monolayer on the membrane. Following the chromogen step and rinses, FrameSlides® were taken immediately to the LCM facility.

Collection of cells using laser microdissection

The system used for laser microdissection was the Positioning Ablation Laser MicroBeam® (PALM®) Micro-Laser system (P.A.L.M. Microlaser Technologies AG, Bernried, Germany). Prior to using the laser, a safety check was done to ensure that the iris diaphragm was open in the epifluorescence beam path, no filters were in the laser

path, the filter block on the unit was set to the "laser" position, and that the FL shutter in the microscope was open according to the operation manual.

Slides were mounted in the PALM® Robostage holding frame. The PALM® CapMover was loaded with three 50-µL LPC-Microfugetubes (P.A.L.M. Microlaser Technologies AG, Bernried, Germany) each with 20 µL of RNAlater® (Applied Biosystems/Ambion, Austin, TX) added to the inside of the cap. The RoboMover® software was used to indicate into which cap the specimen would be collected, and the sample was observed under light microscopy using the Zeiss Axiovert 200M (Zeiss, Germany) microscope attached to the PALM® system.
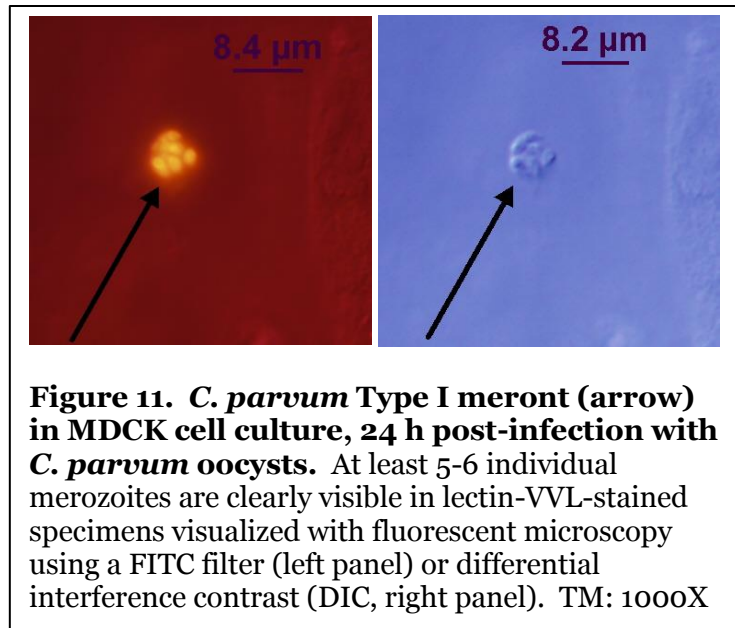
Using a non-essential area on the slide, laser focus and energy was optimized. To determine the laser settings, a zig-zag line was drawn on the screen using the freehand tool. The nitrogen (337 nm) laser was fired, and as it moved along, the focus was adjusted up and down in the plane of the specimen to focus the beam (narrowest cut path). Once focus was determined, energy was reduced and the process was repeated. The ideal energy yields a very narrow, neat line which stops working as soon as the focus is adjusted up or down at all. Ideal laser focus and energy for cutting and catapulting were determined with glass slides and FrameSlides® with MDCK monolayers. Table 5 lists the settings used for these experiments.

The lectin-VVL-prepared slides were observed using a fluorescein isothiocyanate (FITC) filter. Labeled *C. parvum* cells were marked using the system software and cells were removed by laser dissection and catapulted into the microfuge tube cap. Both the rectangle tool and the autocircle tool in the PALM® software were used to mark the areas of interest and catapult the samples into the collection tube.

Table 5. Laser settings on PALM® system for MDCK monolayer slides

Slide Material / Objective	Cut		LPC®	
	Energy	Focus	Energy	Focus
Glass slide, 40X	45	16	53	8
Glass slide, 63X	46	25	55	10
FrameSlide®, 20x	43	57	70	60
FrameSlide®, 40X	44	50	65	51
FrameSlide®, 63X	51	36	73	52

The FrameSlides® were labeled using IHC and were observed under light microscopy to label *C. parvum* cells. Rectangular sections were cut and catapulted in sizes ranging from 10 x 10 μm to 86 x 86 μm. Rectangles were marked in areas that had 4-8 *C. parvum* cells each. The autocircle function was used to cut and catapult individual *C. parvum* cells. Separate tubes were collected containing approximately 50, 100 and 300 *C. parvum* cells. These cells were pelleted by microcentrifugation, and RNA was extracted using and RNeasy™ kit (QIAGEN) according to manufacturer's instructions. All required filters and buffer solutions were provided in the kit. Concentration of RNA for each sample was measured using an ND-1000 spectrophotometer (Nanodrop®, Wilmington, DE). RNA was stored at -80°C following extraction.

Figure 11. ***C. parvum* Type I meront (arrow) in MDCK cell culture, 24 h post-infection with *C. parvum* oocysts.** At least 5-6 individual merozoites are clearly visible in lectin-VVL-stained specimens visualized with fluorescent microscopy using a FITC filter (left panel) or differential interference contrast (DIC, right panel). TM: 1000X

Results

Fluorescent staining of in vitro infections of MDCK cells by C. parvum

Fluorescent microscopy, utilizing a FITC filter, and differential interference contrast (DIC) microscopy were used to observe the Lectin-VVL-stained C. parvum on chamber slides. Oocysts, Type I meronts, Type II meronts, and merozoites were observed. Intracellular meronts were identified, and individual merozoites were visible within the meront. Type I meronts were readily identified, as 6-8 merozoites could be visualized (Figure 11, left panel). The same meront observed under fluorescent microscopy was also observed with DIC microscopy surface morphology was observed (Figure 11, right panel). Type II meronts were difficult to identify, since the differences in the visual plane made counting the four merizoites very challenging. Figure 12 shows a DIC image of a Type II meront.

Merozoites that had only partially erupted from the parasitophorous vacuole were observed. By using a combination of DIC and fluorescence, an image showing the glowing merozoites along with surface structure and detail was captured (Figure 13).

Fluorescence staining on FrameSlides® required leaving out the steps using Slow Fade, due to the interference it would cause with the laser microdissection. Initially, the *Cryptosporidium* cells were visible under fluorescence microscopy, but quickly faded before there was time to capture cells.
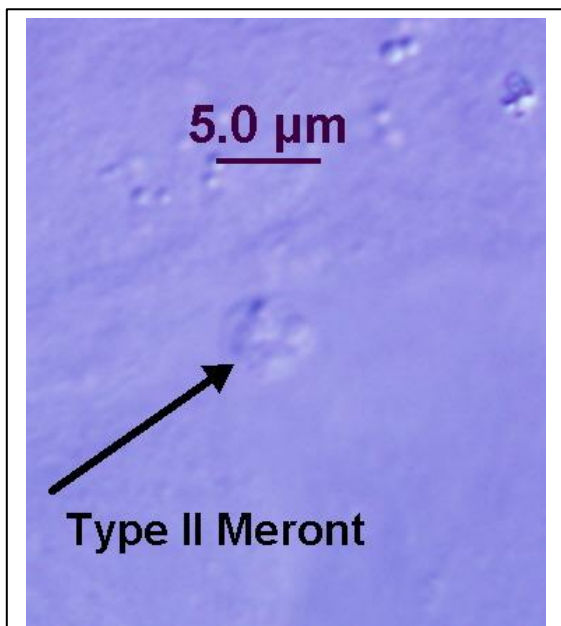

Figure 12. Type II meront in MDCK cells culture, 24 h post-infection with *C. parvum*. Differential interference contrast (DIC) microscopy shows four individual merozoites in a single oocyst.
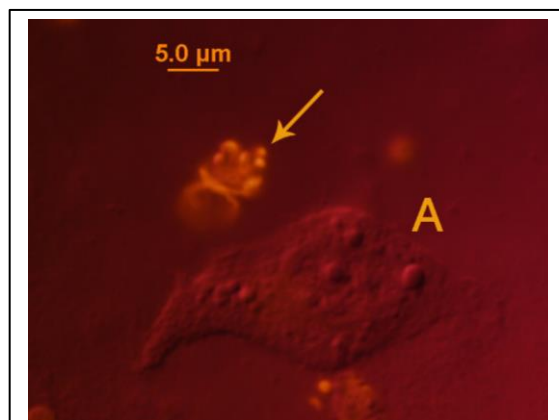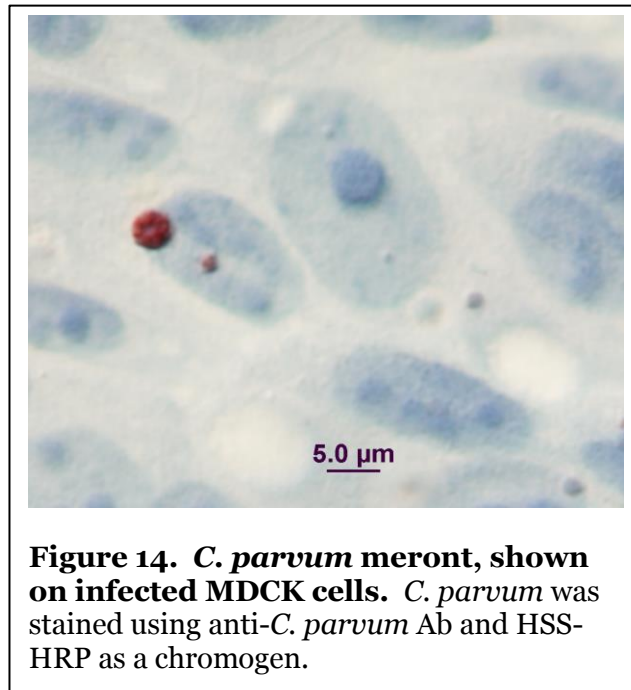

Figure 13. MDCK cell with erupting merozoites. A combination of fluorescence and DIC microscopy show morphology of a MDCK cell (A) and a meront with erupting merozoites (arrow).

*Immunohistochemical staining with anti-*C. parvum *Ab.*

The Ab showed clearly against the background of MDCK cells. These were

counterstained with a 1-s dip in hematoxylin (Figure 14). Very little non-specific staining

was observed. IHC staining on FrameSlides® was effective for use with the PALM system,

as the stain was easily visible onscreen and didn't fade with light.

Figure 14. *C. parvum* meront, shown on infected MDCK cells. *C. parvum* was stained using anti-*C. parvum* Ab and HSS-HRP as a chromogen.

Capture of C. parvum *cells via laser microdissection*

RNA was extracted from the batches of cells captured via LCM™. Tubes containing

50, 100, and 300 *C. parvum* meronts yielded 11.0 ng/µL, 10.4 ng/µL, and 8.5 ng/µL of

RNA in 10 µL of RNA solution, respectively. Unfortunately, this did not equate to

quantities that were large enough to successfully identify *C. parvum* by PCR.

Discussion

LCM™ provides enormous opportunities for cellular and genetic research in many

fields. Combined with monoclonal antibody labeling techniques, a number of specific cells

or structures can be differentially labeled and separated for analysis. Breakthroughs in criminal investigation lend some insight into the possibilities open to a multitude of research fields. Currently, forensic analysts can use Y chromosome-specific markers from a small sample, allowing them to find and capture sperm cells from a swabbed slide (Elliot, et al., 2003). Applying the same type of selective labeling, researchers can isolate specific populations of cells or substances and use genetic analysis on close-to-pure samples of DNA or RNA.

Cryptosporidium research has many facets that remain largely unexplored; due to the relatively short time it has been of clinical interest. One aspect that is particularly interesting is understanding the trigger that causes the parasite to switch from asexual reproduction for replication within a host to sexual reproduction and passage of oocysts from the host. Since it is thought that Type II meronts precede gametogony, the ability to cull only Type I or Type II meronts from an infected tissue sample or cell culture sample would allow comparison for differential gene expression. Understanding the trigger for the switch could provide information for development of chemotherapy or vaccination to prevent the spreading of the parasite.

While all of the functions aren't fully clear yet, it is accepted that the genes for *Cryptosporidium* Oocyst Wall Proteins *(COWP1-8)* play an important role in the sexual reproduction of *Cryptosporidium.* These proteins are exclusively located in the oocyst walls, so being able to detect up regulation of the genes could signal the switch to sexual reproduction. Using LCM™ to selectively collect Type I and Type II meronts for comparative analysis could lead to detection of Type-specific markers to positively identify meronts and the stage of the life cycle the parasite is in.

The development of cell culture techniques directly on FrameSlides® for infection studies is a big step. New staining techniques that overcome the shortcomings of the current techniques are needed to assist in this endeavor. While one-step fluorescent

labeling is possible, the fast fading of the fluorescence limits functionality of these for LCM™. IHC techniques specifically label *Cryptosporidium* cells, but the process itself seems to be damaging to RNA, which prevents analysis of gene expression. Development of a one or two-step chromogenic stain could be the solution and is one possible direction to follow. Development of water-free IHC techniques could limit the reactivation of endogenous RNases, which is a possible cause of the RNA damage (Tangrea, et al., 2001).

Another possibility worth exploring would be to see if Liquid Cover Glass (Zeiss, Germany) would be useful in fluorescent staining for LCM. This is designed to be used in conjunction with the P.A.L.M.™ system, so LCM™ is possible with the product on samples. Whether the fluorescent signals would persist long enough for location and collection of cells would need to be determined.

The problem of low yield of RNA could also be addressed with improved RNA amplification. It is possible to amplify the RNA from a single cell, using of commercial kits (Lang, et al., 2009). However, the kits are quite expensive and would not address the issue of RNA damage caused by IHC. Utilization of some form of RNA amplification would be likely to improve LCM™ results.

Acknowledgements

References

Casemore, D.P., Armstrong, M., Sands, R.L., 1985. Laboratory Diagnosis of cryptosporidiosis. J. Clin. Pathol. **38**, 1337-1341.

Elliott, K., Hill, D.S., Lambert, C., Burroughes, T.R., Gill, P. 2003. Use of Laser Microdissection Greatly Improves the Recovery of DNA From Sperm on Microscope Slides. Forensic Sci. Int. **137**, 28–36

Guerrant, R.L., 1997. Cryptosporidiosis: an emerging, highly infectious threat. Emerg. Infect. Dis. **3**, 51.

Lang, J.E.,Magbanua, M.J.M, Scott, J.H., Makrigiorgos,G.M., Wang, G., Federman, S., Esserman, L.J., Park, J.W., Haqq, C.W. 2009. A Comparison of RNA Amplification Techniques at Sub-Nanogram Input Concentration. BMC Genomics. **10,** 326-337.

Liu, J., Deng, M., Lancto, C. A., Abrahamsen, M. S., Rutherford, M. S., Enomoto, S., 2009. Biphasic modulation of apoptotic pathways in *Cryptosporidium parvum*-infected human intestinal epithelial cells. Infect. Immun., **77**, 837-49.

Liu, J., Enomoto, S., Lancto, C.A., Abrahamsen, M.S., Rutherford, M.S., 2008. Inhibition of apoptosis in *Cryptosporidium parvum* infected intestinal epithelial cells is dependent on survivin. Infect. Immun. **76,** 3784–3792.

Plattner, Fabienne and Dominique Soldati-Favre. 2008. Hijacking of host cellular

functions by the apicomplexa. Annu Rev Microbiol **62**:471-87

**Tangrea, M.A., Mukherjee, S., Gao, B., Markey, S.P., Du, Q., Armani, M.,

Kreitman, M.S., Rosenberg, A.M., Wallis, B.S., Eberle, F.C., Duncan,

F.C., Hanson, J.C., Chuaqui, R.F., JRodriguez-Canales, J., Emmert-

Buck M.R**. 2001. Effect of Immunohistochemistry on Molecular Analysis of

Tissue Samples: Implications for Microdissection Technologies. Journal of

Histochemistry & Cytochemistry. **59,** 591–600.

CHAPTER 3: TIME SERIES INFECTION IN MDCK CELLS TO STUDY SHIFT FROM ASEXUAL TO SEXUAL REPRODUCTION

Introduction

Cryptosporidiosis is a parasitic, diarrheal disease caused by the apicomplexan *Cryptosporidium*. The disease is of clinical concern as immunocompromised patients may develop chronic diarrhea that may have fatal consequences (Casemore, 1985, Guerrant, 1997). The disease is typically contracted through contaminated recreational or drinking water. The infectious oocysts withstand chlorination; so can be persistent, even in treated water (Fayer, et al., 2000, Casman, 2000).

Cryptosporidium parvum is one of two species that most frequently cause human cryptosporidiosis: the other is *Cryptosporidium hominis* (Ernest, et al., 1986, Zu, et al., 1992). *C. parvum* has a complicated life cycle that includes an environmental infectious stage consisting of infectious oocysts being shed in the feces of hosts. Once ingested, the parasite typically establishes infection in the small intestine. Within the host, there are two types of reproduction. Asexual reproduction, merogony, in which repeated generations of Type I meronts produce merozoites that infect other cells within the host occurs first. Type II meronts, which are thought to produce merozoites that develop into gametes and oocysts are formed. The trigger for switching from asexual to sexual reproduction is not understood for *Cryptospordium* (Current and Reese, 1986). For some of the apicomplexans, there are a certain number of generations of merogony before sexual reproduction begins. In others, such as malaria, there is a coordination based on time of generation cycles (McDougald and Jeffers, 1979).

Oocysts are of two forms. Thin-walled oocysts seem to function to perpetuate the infection in a single host through autoinfection. Thick-walled oocysts are shed in the feces,

are very resistant to many environmental conditions, and are infectious to new hosts (Current and Reese, 1986, Current and Garcia, 1991).

Although the mechanism by which *C. parvum* switches its reproductive cycle has not been elucidated, a possible trigger may be the availability of fresh host cells to infect. Our hypothesis for this study was that merogony continues as long as there is an available source of uninfected cells for the merozoites to enter. Once the cells in an area of the intestine–or experimentally, in the cell culture flask–have been saturated, sexual reproduction allows for migration out of the host or to a new area of host tissue for autoinfection.

In order to explore the effect of host-cell availability on the timing of the life cycle, a series of infections was carried out using variations in cell confluency and variations in inoculation size to simulate high- and low-density infections. Then, the transcription of genes that produce life stage marker proteins was assessed. The marker used for early life cycle was the actin gene, since actin rearrangement is a part of the initial invasion process (Sibley, 2004, Abrahamsen and Schroeder, 1999). The *18S* small subunit ribosomal RNA (SSU rRNA) was used as a housekeeping gene to track that *Cryptosporidium* cells were actively growing. Production of oocysts signals that sexual reproduction has occurred, so, to test for the presence of sexual life stages, upregulation of the genes encoding *Cryptosporidium* oocyst wall proteins (*COWP1* and *COWP8*) was measured. qPCR analysis was used to determine time points at which each gene was being expressed, as well as a relative measure of the degree of upregulation.

Materials and methods

Comparison of temporal gene expression from high- and low-density C. parvum *infections on Chamber Slides®*

      To compare the expression of various life cycle-related genes under different growth conditions, an infection series was set up to have simultaneous infections with high and low numbers of oocysts and high and low host-cell density. This allowed comparison of the impact of host cell density and oocyst infectious dose.

      To ensure slides with the target confluency of 50% and 90% would be available, a range of concentrations was used to seed chamber cells. Twenty-four chamber slides, in sets of six, were seeded at the following concentrations of MDCK cells (cells/mL): 1.7×10^5, 1.5×10^5, 1.0×10^5, and 0.9×10^5 in MEM plus 10% FBS (Appendix). These were incubated at 37°C with 5% CO_2 in a humidified chamber for 24 h. The slides were observed to determine confluency. The chamber slides that were approximately 50% confluent and approximately 90% confluent were chosen for the high- and low-density time series. Time points were 2 h post-infection (hpi), 6 hpi, 12 hpi, 24 hpi, 48 hpi, and 72 hpi. The chambers on each slide were inoculated with varying numbers of *C. parvum* oocysts: 320,000; 100,000; 10,000; and 1000 oocysts in infection medium.

      C. parvum (Iowa isolate) oocysts were obtained (Waterbourne, Inc., New Orleans, LA). Oocyst concentration was 6.25×10^5/mL in PBS with 1 mM Sigma A5955 antibiotic/antimycotic. For each well, the appropriate volume of the oocyst suspension was added to a 1.5-mL centrifuge tube (5×10^4 oocysts/well). The tubes were centrifuged at 20,000 $\times g$ for 3 min. The oocysts were resuspended in 200 μL of 10% bleach solution and incubated for 10 min at 4°C. Following this incubation, cells were centrifuged at 20,000 $\times g$ for 3 min and the supernatant was removed. Oocysts were washed in sterile PBS three times. Washes were carried out by adding 200 μL sterile PBS, vortexing to

resuspend, centrifuging at 20,000 $\times g$ for 3 min, and removing supernatant. Oocysts were resuspended in 500 μL of 0.8% sodium taurocholate (NaTC) and incubated at 37°C for 30 min. This incubation was followed by the same rinse series as the bleach treatment. Oocysts were resuspended in 1 mL of infection medium.

Chamber slides with monolayers of 70-80% confluent MDCK (ATCC CCL-34) cells were removed from the incubator and medium was removed. The infection medium containing the oocysts was added to each well. A negative control well containing only infection medium and uninfected MDCK cells was included. Chamber slides were returned to the CO_2 incubator for 3 h to allow excystation and for the released sporozoites to infect the MDCK cells. Infection medium was removed and 1 mL MEM with 10% FBS was added to each well for incubation.

Cells were incubated for 24-48 h, the growth medium was removed and cells were rinsed twice with 1 mL PBS. To fix cells for staining, 1 mL of 4% formaldehyde was added to each well and allowed to sit for 30 min at room temperature. This solution was removed and cells were washed twice in PBS by adding 1 mL to each well and removing with vacuum apparatus.

These were incubated at 37°C with 5% CO_2 in a humidified chamber. At each time point, one chamber slide from each set was removed from the CO_2 chamber, and the infection medium was removed. RNA was either immediately extracted or 1.0 mL RNAlater™ (QIAGEN, Valencia, CA) was added to the chamber to preserve RNA until extraction.

RNA extraction

Infection medium or RNAlater™ was removed from the wells and 1 mL lysis buffer (Appendix) was added to each well. Cells from each well were scraped off the slides and collected in separate 1.5-mL microcentrifuge tubes. RNA was extracted from each sample

using an RNeasy™ kit (QIAGEN), as per manufacturer's instructions. All required filters

and buffer solutions were provided in the kit. Concentration of RNA for each sample was

measured using an ND-1000 spectrophotometer (Nanodrop®, Wilmington, DE). RNA was

stored at -80°C following extraction.

Synthesis of cDNA

The SMART MMLV® Reverse Transcriptase system (ClonTech, Mountain View,

CA) was used for cDNA synthesis. In addition to the kit components, random primers

(Promega, Madison, WI) and 10 mM dNTP mix (Promega, Madison, WI) were used.

Initially an 11-μL mixture with random primers and extracted RNA was made. This

mixture was heated at 70°C for 3 min to denature the RNA and held at 4°C to allow

annealing of the primers to the RNA.

The master mix contained 4 μL 5x first-strand buffer, 2 μL dNTP mix, and 2 μL 100

mM DTT (total of 8 μL per reaction tube). Eight microliters of master mix was added to

each tube, and 1 μL SMART MMLV or 1 μL RNase-free water (for rt – control). This

mixture was incubated at 42°C for 60 min to allow synthesis of the first strand cDNA. The

reaction was terminated by inactivating the reverse transcriptase at 70°C for 15 min. The

cDNA was stored at -20°C.

qPCR analysis of COWP1, COWP8 and actin *gene expression*

Primers and probes for *COWP1* and *COWP8* were available, but primers and a

probe were needed. Primer and probes were designed for the *C. parvum* actin gene using

Primer Express 2.0 (Applied Biosystems, Carlsbad, CA). A MGB probe with 6-FAM™

fluorophore and primers were obtained from Integrated DNA Technologies (Coralville,

IA). Sequences were verified as *Cryptosporidium* with BLAST; forward primer

CATCCACCGGGTTTAGAGTTG, reverse primer GGGTTGAATGGACAATTAGGGTAT,

probe TCTATCACTGGTCTCCCAAC.

Quantitative real-time PCR (qPRC) was carried out using an ABI 7500 Real-Time PCR machine (Applied Biosystems). The comparative C_T method, using the arithmetic formula $2^{-\Delta\Delta CT}$ was used to calculate the relative fold change in gene expression of *COWP1*, *COWP8* and *actin* using *C. parvum 18S* as the housekeeping gene.

Results

Actin expression

Actin expression levels based on fold-change data from qPCR show peak expression of actin genes occurring at varying time points. Different samples had peak expression at 12 hpi, 24 hpi, and 48 hpi (Figure 15). Three of the samples grown on confluent host cells peaked at three different times. There is no clear relationship between host cell confluency or infectious dose and the expression of actin gene.
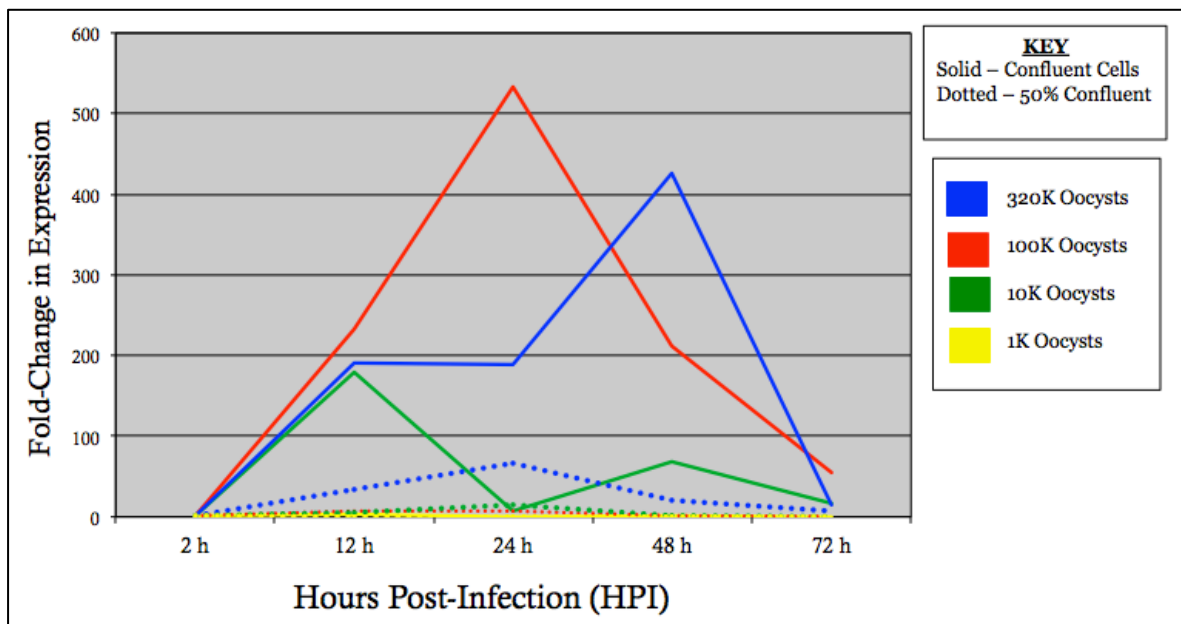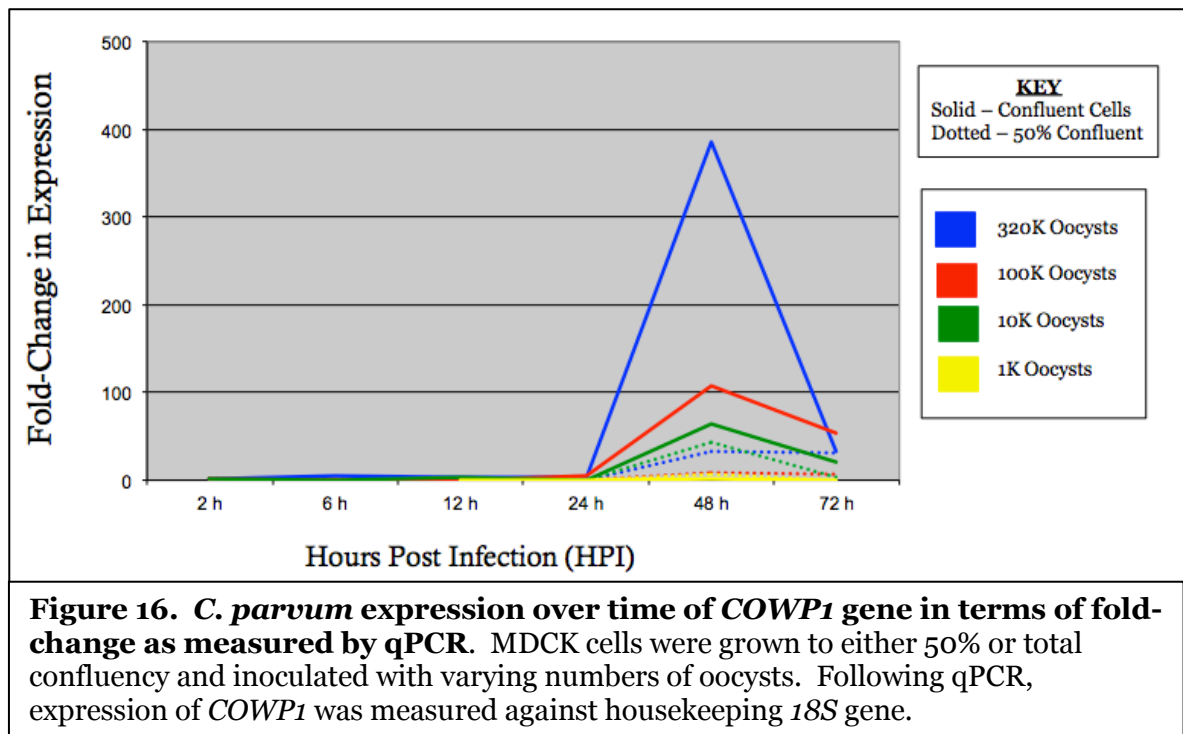

Figure 15. *C. parvum* actin gene expression over time. Gene expression was measured at various infectious doses in cell cultures with either sparse (50% confluent) or confluent growth at the time of infection. Results are reported in terms of fold-change as measured by qPCR, using expression of the *18S* gene as a housekeeping gene.

COWP1 *expression*

qPCR was used to measure *COWP1* gene expression for samples collected over the time series infection. The largest peak in expression was at 48 hpi and expression was downregulated at 72 hpi in all of the samples (Figure 16). During the early part of the infection, up to 24 hpi, there was low-level detection of *COWP1* expression in the samples that had been exposed to larger doses of oocysts, however this was at very low levels when compared to the peak expression at 48 hpi.

Expression was upregulated and then downregulated early on in three of the samples grown on confluent MDCK cells. The changes in expression are not substantial when compared to the later peak expression (Figure 17).

Figure 16. *C. parvum* expression over time of *COWP1* gene in terms of fold-change as measured by qPCR. MDCK cells were grown to either 50% or total confluency and inoculated with varying numbers of oocysts. Following qPCR, expression of *COWP1* was measured against housekeeping *18S* gene.

COWP8 *expression*

COWP8 expression, based on qPCR analysis, peaked at 72 hpi in 7 of the 8 groups tested. Only the sample from the confluent host cells with 320 thousand oocyst infectious

dose peaked earlier than that, at 48 hpi (Figure 18). Three of the infected cultures using

confluent host cells showed low levels of expression *COWP8* at both 6 hpi and 12 hpi

(Figure 19). Expression dropped off completely by 24 h. With the exception of the sample

with confluent host cells infected with 320,000 oocysts, expression sharply increased at 48

hpi and was still prominent at 72 hpi. The samples with very high infectious doses had an

increase in expression of the *COWP8* gene at 6 hpi with downregulation at 12 hpi, with no

expression detected at 24 hpi. These samples had much higher expression later in the

infection, at 48 hpi and 72 hpi.

**Figure 17. Graph showing *C. parvum* expression over time of *COWP1*
during the first 24 hpi.** MDCK cells grown either to 50% confluency or 100%
confluency were infected with varied numbers of oocysts. The expression of the *COWP1*
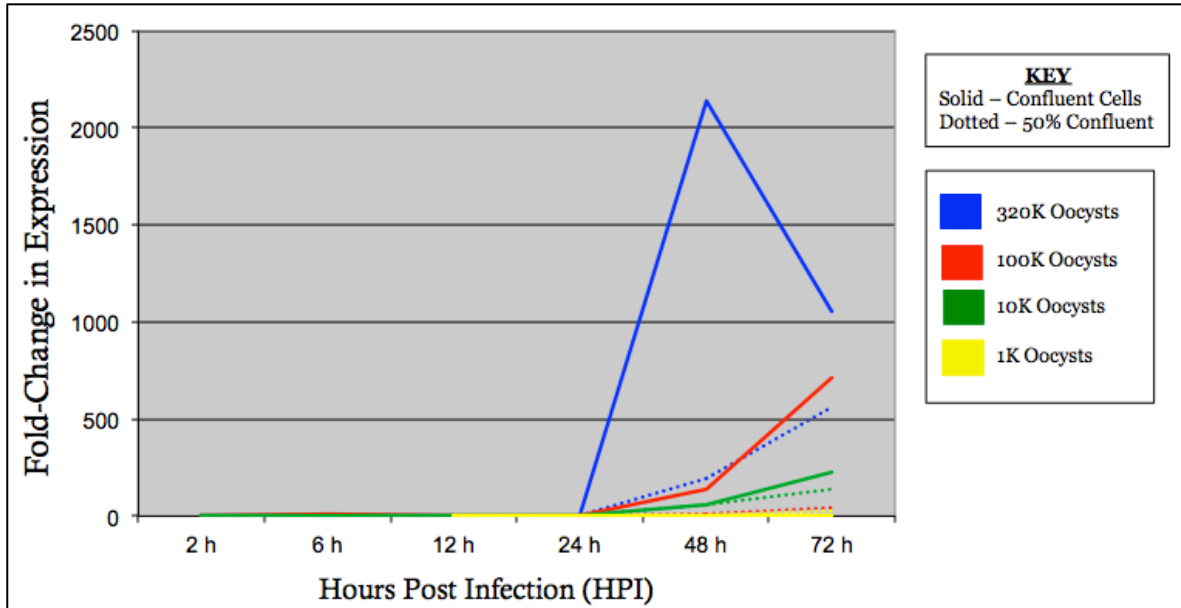gene during the first 24 hours hpi is shown.
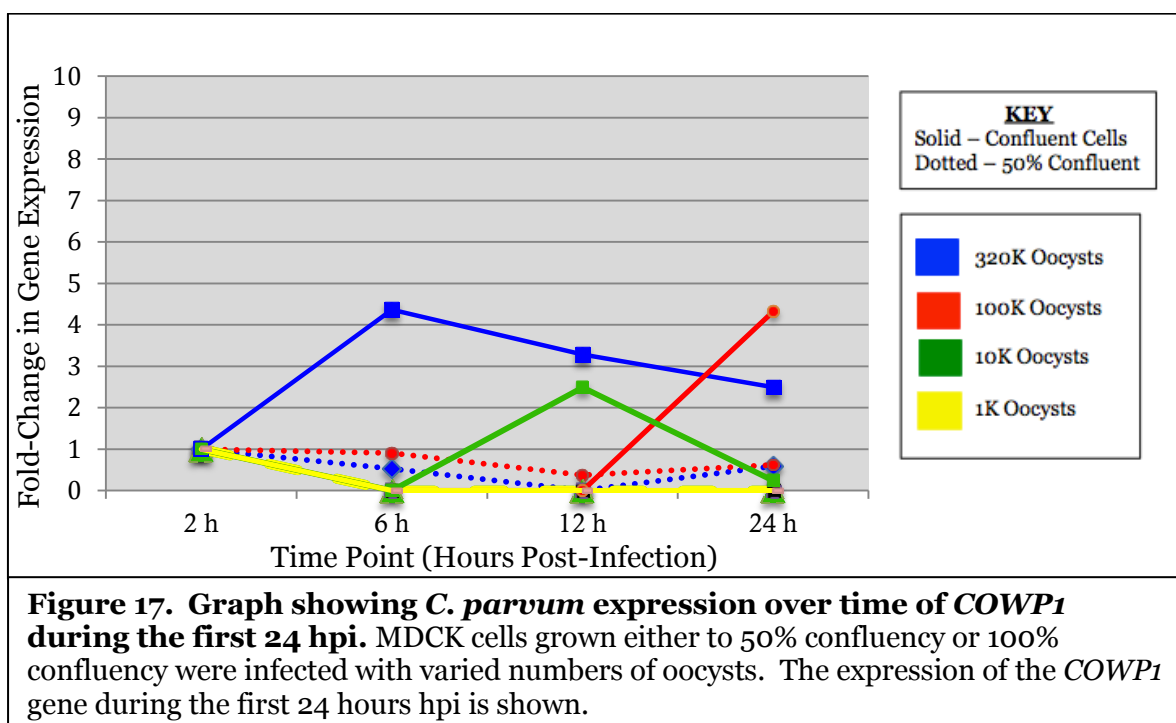
Figure 18. *C. parvum COWP8* gene expression over time (fold-change as measured by qPCR). MDCK cells grown to either 50% or 100% confluency were inoculated with a range of infectious does of oocysts and *COWP8* expression was measured at various time points following infection using qPCR and *18S* as a housekeeping gene.

Discussion

In order to create conditions with varying availability of fresh host cells to be infected, we employed two approaches that varied in the number of targets and the number of infectious agents. The number of host cells that were initially available could be limited by infecting cell culture flasks that had been grown to only 50-60% confluency. The number of oocysts in the infectious dose were also varied to give high- or low-density infections. Various pilot infection series showed that using cell cultures with less than 60% confluency did not result in productive infections (data not included). The data for the series using low-confluency host cells was inconsistent and even the *18S* housekeeping gene could not be detected in some of the samples. The experiments using confluent host cells for infections with varying inoculum sizes did yield measurable results, which we
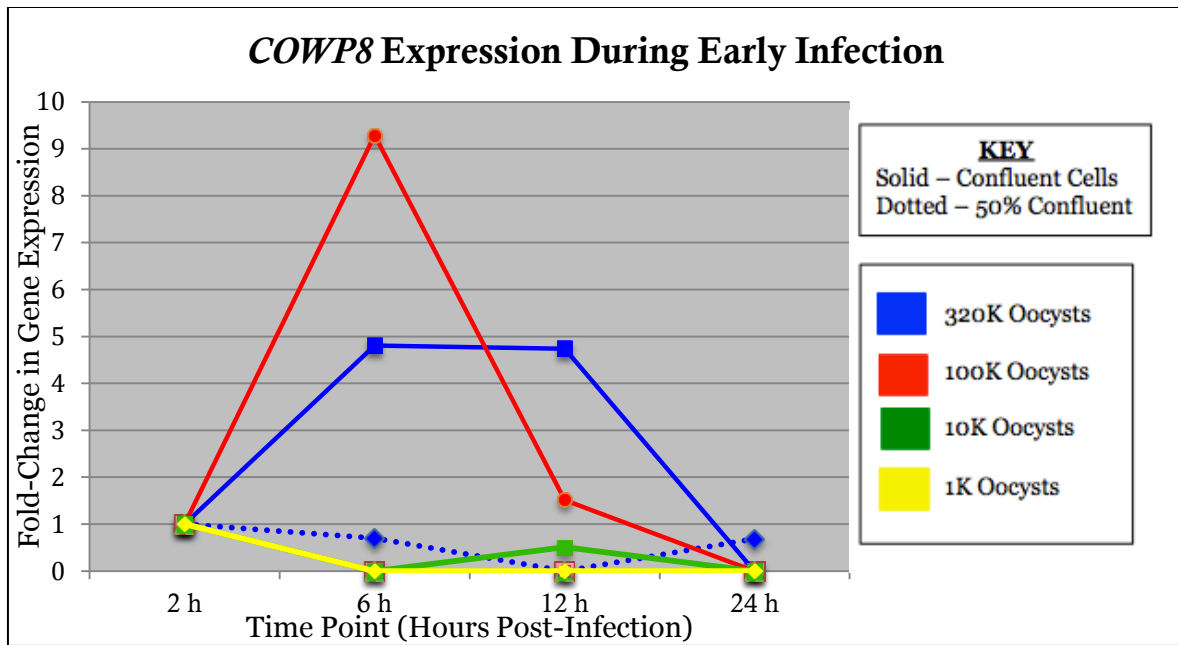
Figure 19. Expression of *C. parvum* COWP8 gene (fold-change as measured by qPCR). MDCK cells grown to either 50% or 100% confluency were inoculated with a range of infectious does of oocysts and *COWP8* expression was measured at various time points following infection using qPCR and *18S* as a housekeeping gene. Expression during the first 24 hpi are shown.

were able to analyze. Our original hypothesis was disproven. Our results indicate that there is not an apparent relationship between the availability of cells to infect and the switch to sexual reproduction. The infections that started with very low numbers of oocysts switched to sexual reproduction at the same time point as the infections that were started with 320,000 oocysts, using the expression of *COWP1* and *COWP8* as a measure of sexual development. Although our hypothesis was not supported, our results add to the body of knowledge of things that do not trigger the switch to sexual production.

The use of actin as an early life-stage marker does not appear to be a good choice. Its expression did not have consistent timing for any of the experiments. This makes sense if actin remodeling is used for motility, since there are multiple rounds of merogeny, the actin gene would be expressed at more than one time, and not necessarily downregulated when sexual reproduction is beginning to take place. One possible future use of

93

monitoring the actin gene would be to measure the length of time each cycle of merogeny takes, if actin is upregulated for infection and then downregulated during cell division.

There are still not a large number of studies looking at the expression of the various genes of *C. parvum* over time, and the existing studies leave large gaps. Data for 6, 12, 24, 48, and 72 hpi are readily available, but little can be found for other times. Considering that our data shows peak production at 24 and 48 hpi for some of these genes, it could be helpful to know in more detail the times for activation. A series of experiments using three- or six-hour intervals for up to 96 hours could be very useful in elucidating the timing of the regulation of the various COWP genes. It may be that there is a particular sequence that is not being seen due to the large time gaps between sampling.

References

Abrahamsen, M.S., Schroeder, A.A. 1999. Characterization of Intracellular *Cryptosporidium parvum* gene expression. Mol. Biochem. Parasitol. **104**, 141-146.

Casemore, D.P., Armstrong, M., Sands, R.L., 1985. Laboratory Diagnosis of cryptosporidiosis. J. Clin. Pathol. **38**, 1337-1341.

Casman, E.A., Fischhoff, B., Palmgren, C., Small, M.J., Wu, F., 2000. An integrated risk mode of a drinking-water-borne Cryptosporidiosis outbreak. Risk Analy. **20**, 495-511.

Current, W. L., L. S. Garcia., 1991. Cryptosporidiosis. Clin. Microbiol. Rev. **4**, 325-358.

Current, W. L., N. C. Reese, 1986. A comparison of endogenous development of three

isolates of *Cryptosporidium* in suckling mice. J. Protozool. **33**:98–108.

Fayer R., Morgan, U., Upton, S. J., 2000. Epidemiology of *Cryptosporidium*:

transmission, detection and identification. Int. J. Parasitol. **30**, 1305-22.

Guerrant, R.L., 1997. Cryptosporidiosis: an emerging, highly infectious threat. Emerg.

Infect. Dis. **3**, 51.

James A. Ernest, Byron L. Blagburn, David S. Lindsay, William L., 1986.

Infection dynamics of *Cryptosporidium parvum* (Apicomplexa: cryptosporiidae) in

neonatal mice (*Mus musculus*). J. Parasitol. **72**, 796-798.

McDougald L. R., and Jeffers T. K., 1976. *Eimeria tenella* (Sporozoa, Coccidia):

Gametogony following a single asexual generation. Science **192**: 258-259.

Sibley, L.D., 2004. Intracellular parasite invasion strategies. Science **304**, 248–253.

GENERAL DISCUSSION

Many aspects of cryptosporidiosis are still poorly understood; this is at least partially due to the difficulty of long-term laboratory propagation of the organism. The complex life cycle of *Cryptosporidium* and the lack of knowledge of specific details of the different stages of the life cycle provide not just difficulties for research, but many opportunities of exploration to increase the understanding of this important zoonotic pathogen. Understanding *Cryptosporidium* is necessary due to the implications of these infections in public health. Immunocompromised patients and outbreaks caused by municipal and recreational water contamination provide the impetus to further study this organism.

Improving the ability to identify specific life stages, through staining techniques and microscopy can allow selective harvesting of cells in the same life stage, allowing genetic and cellular structure analysis. These studies then can lead to creating better molecular markers for study of infections. Due to the unique niche that the organism occupies within host cells, the mechanisms for triggering immune responses is not known. Specific labeling of life cycles within infected cells, coupled with surveys of the type of immune cells being activated could provide insight. In addition, the development of receptors for specific cell structures opens the door to better chemotherapy for an infection that has, thus far, mostly eluded pharmaceutical intervention.

Use of cell culture FrameSlides™ may enable a more accurate collection of cells for research. However, until immunohistochemical staining techniques that are less prone to activating intrinsic RNases can be developed, RNA analysis from cells collected this way will be limited. The challenge is that existing commercial stains that are fluorescent need some sort of cover to keep the signal from being quenched, while laser microdissection requires that the cells be exposed for removal. This would provide an excellent focus for a

project, attempting to reduce RNases during IHC to enable RNA analysis from laser microdissection-collected cells.

Laser microdissection is a tool that should prove useful in pursuing immunological study of *Cryptosporidium* infections. Utilizing a mouse model for infection, tissue sections can be mounted on either FrameSlides™ or glass slides with the proper membranes for use with a laser for microdissection. Cells in the area of infected cells could be studied, as well as the presence of various cytokines from activated immune cells. Being able to carefully cut away the cells adjacent to an infected cell provides the opportunity to study the response of host tissue to infection.

Although the time series study disproved our hypothesis, a much more in-depth time series would be invaluable to study the timing of the activation of particular genes. Our study was limited in order to create a high-density infection, but could be repeated with confluent cell cultures for a higher yield for a higher yield of *Cryptosporidium*. An in-depth time series utilizing checks every three hours, instead of six, and using multiple host cells lines could provide data on the activation of different genes and demonstrate if the life cycle is driven by the type of host cell the parasite has infected.

Another possible avenue that could be pursued would be that if a person is able to pull out cells infected with *Cryptosporidium*, it could be possible to try to figure out what antigens are being presented on the surface of the infected cells. Knowing the structures that are antigenically significant could provide a direction for treatment or prevention.

Overall, these experiments have helped demonstrate the vast array of possibilities for further study and the complexity of the organism that causes cryptosporidium.

APPENDIX

Media recipes

Infection media

5 mL   10% Opti-MEM (Gibco BRL)

5 mL   10% Fetal Bovine Serum

500 μL   1x antibiotic/antimycotic solution (Sigma, 100x 10,000 units penicillin, 10 mg streptomycin, 25 μL amphotericin B/mL)

500 μL   1 mM sodium pyruvate (Sigma)

0.4515 g   50 mM glucose

87.5 μL   35 μg/mL ascorbic acid, stock solution 20mg/mL (Sigma)

100 μL   1.0 μg/mL folic acid, stock solution 0.5 mg/mL (Sigma)

100 μL   4.0 μg/mL 4-aminobenozoic acid, stock solution 2 mg/mL (Sigma)

10 μL   2.0 μg/mL calcium pantothenate, stock solution 10 mg/mL (Sigma)

38.702   Minimum Essential Medium Eagle with Earl's salts, L-Glutamine, non-essential amino acids, without $NaHCO_3$ (Gibco)

pH to 7.4 with 1 M NaOH or 1 M HCl

Filter sterilize with 0.22 micron filter

Trypan blue solution in Hank's balanced salt solution

0.4 g   Trypan Blue (Sigma)

100 mL   Hank's Balanced Salt Solution, HBSS (Sigma)

Working Stock Solution

0.2 mL   0.4% Trypan Blue in HBSS

0.8 mL   HBSS

PBS buffer

80.0 g   NaCl

11.6 g Na_2HPO_4

2.0 g KH_2PO_4

2.0 g   KCl

~9.8 L   Deionized water (bring volume to 10.0 L)

pH to 7.0 with 1.0 M HCl or 1.0 M NaOH

Bleach solution

100 mL   Chlorox ® Bleach

900 mL   Deionized water

Store at 4°C

Sodium taurocholate solution

0.8 g   Sodium taurocholate (Sigma)

100 mL   PBS buffer

Filter sterilize with 0.22 micron filter

1X TAE buffer solution

50 mL   50X TAE buffer solution (Sigma)

950 mL   Deionized water

Store at 4°C

Trypsin solution

2.5 g	Trypsin (Gibco)
8.0 g	NaCl
0.06g	Na_2HPO_4
0.2 g	EDTA
0.4 g	KCl
1.0 g	Dextrose
950 mL	Deionized water

Bring volume to 1 L with deionized water.

Lysis buffer

10 μL	Beta-mercaptoethanol (Sigma)
1.0 L	Buffer RLT plus from RNeasy ™ kit (QIAGEN)

Mix immediately prior to RNA extraction